BIOPHYSICAL STUDIES OF PROGESTERONE-MODEL MEMBRANE
INTERACTIONS

A THESIS SUBMITTED TO
THE GRADUATE SCHOOL OF NATURAL AND APPLIED SCIENCES
OF
THE MIDDLE EAST TECHNICAL UNIVERSITY

BY

FİLİZ KORKMAZ

IN PARTIAL FULFILLMENT OF THE REQUIREMENTS FOR THE DEGREE
OF MASTER OF SCIENCE
IN
IN DEPARTMENT OF PHYSICS

SEPTEMBER 2003

Approval of the Graduate School of Natural and Applied Science

_____

Prof. Dr. Canan ÖZGEN

Director

I certify that this thesis satisfies all the requirements as a thesis for the degree of Master of Science.

_____

Prof. Dr. Sinan BİLİKMEN

Head of the Department

This is to certify that we have read the thesis and that in our opinion it is fully adequate, in scope and quality, as a thesis for the degree of Master of Science.

_____   _____

Prof. Dr. Feride SEVERCAN   Prof. Dr. Halil KIRBIYIK

Co-Supervisor   Supervisor

Examining Committee Members

Prof. Dr. Halil KIRBIYIK   _____

Prof. Dr. Feride SEVERCAN   _____

Prof. Dr. Sinan BİLİKMEN   _____

Prof. Dr. Nadide KAZANCI   _____

Prof. Dr. Belma TURAN   _____

ABSTRACT

BIOPHYSICAL STUDIES OF PROGESTERONE-MODEL MEMBRANE INTERACTIONS

Korkmaz, Filiz

M. S. Department of Physics

Supervisor: Prof. Dr. Halil Kırbıyık

Co-Supervisor: Prof. Dr. Feride SEVERCAN

September 2003, 143 pages

Interactions of progesterone with zwitterionic dipalmitoyl phosphotidylcholine (DPPC) multilamellar liposomes (MLVs) were investigated as a function of temperature and progesterone concentration by using three non-invasive techniques of Fourier transform infrared (FTIR) spectroscopy, turbidity at 440 nm and differential scanning calorimetry (DSC).

The results show that 1mol% of progesterone does not induce a significant change in the shape of thermotropic profile of DPPC. However as progesterone concentration increases, the main transition temperature decreases and phase transition curve broadens. Higher concentrations (12, 18 and 24mol%) also decreased the transition temperature but not as significantly as lower concentrations. The characteristic pretransition of DPPC was completely disappeared upon the addition of progesterone. Progesterone disorders the phospholipid membranes in a concentration dependent manner. Furthermore, low concentrations of progesterone (3, 6 and 9mol%) increase the fluidity of the system but high concentrations (12, 18 and 24mol%) stabilize the membranes by decreasing the mobility of the acyl chains. The opposite effect of progesterone on membrane dynamics of low and high concentrations was also supported by turbidity studies at 440 nm.

DSC peaks broaden and shift to lower temperature degrees with increasing concentrations up to 9mol% of progesterone. At 6 and 12mol% of progesterone, the curve contains more than one peak. This indicates the existence of phase separation. The pretransition of liposomes was eliminated for all samples containing progesterone.

Analysis of C=O stretching bond in FTIR spectroscopy showed that progesterone does not make any hydrogen bonds with the interfacial region of DPPC liposomes, instead it induces free carbonyl groups in the system. Ester groups were found to be disordered by the addition of progesterone and the effect is profound with 6 and 9mol% concentrations.

The head group of liposomes were found to make hydrogen bonding in the vicinity of 3mol% of progesterone in both phases and of 6mol% of progesterone in liquid crystalline phase by infrared spectroscopy of PO_2^- stretching mode. This hydrogen bonding is made either with the hydroxyl group of progesterone or with the water molecules around the head group. With other concentrations of progesterone, there is no evidence of hydrogen bond formation.

ÖZ

PROGESTERONUN MODEL MEMBRANLARLA ETKİLEŞMESİNİN BİYOFİZİKSEL YÖNTEMLERLE İNCELENMESİ

Korkmaz, Filiz

Yüksek Lisans, Fizik Bölümü

Tez Yöneticisi: Prof. Dr. Halil Kırbıyık

Ortak Tez Yöneticisi: Prof. Dr. Feride SEVERCAN

Eylül 2003, 143 sayfa

Bu tezde progesteronun dipalmitol fosfatidilkoline'den (DPPC) oluşan çok katmanlı lipozomların termotropik faz davranışı ve fiziksel özelliklerine olan etkisi, katman yapısına zarar vermeyen üç teknikle, yani; Fourier Transform Infrared (FTIR) spektroskopi, 440 nm de törbiditi tekniği ve diferansiyel tarama kalorimetresi tekniği (DSC) kullanılarak incelendi.

Sonuçlarımız, 1mol% progesteronun DPPC'nin termotropik profilinin şeklinde önemli bir değişikliğe neden olmadığını göstermiştir. Bunun yanısıra, progesterone derişimi yükseldikçe, ana faz geçiş sıcaklığı düşmüş ve faz geçiş eğrisini genişlemiştir. Yüksek konsantrasyon değerlerinde ise (12, 18 ve 24mol%) geçiş sıcaklığı, düşük konsantrasyonlar kadar olmasa da, düşmüştür. DPPC'nin önfaz geçişi, progesteronun eklenmesiyle tamamen yok olmuştur. Progesteron, konsantrasyona bağlı olarak, fosfolipit membranlarının düzenini değiştirmiştir. Progesteronun düşük konsantrasyonları (3, 6 ve 9mol%) sistemin akışkanlığını artırmış fakat yüksek konsantrasyonları (12, 18 ve 24mol%) membranın asil zincirinin hareketliliğini azaltarak stabile etmiştir. Progesteronun alçak ve yüksek konsantrasyonlarda membran dinamiği üzerindeki zıt etkisi 440 nm de törbiditi çalışması ile de desteklenmiştir.

DSC bantları, progesteronun 9mol%'e kadar artan değerleri için genişlemiş ve daha düşük sıcaklık değerlerine kaymıştır. 6 ve 12mol% progesteron değerlerinde, eğri birden fazla bant içermektedir. Bu da faz ayrılmasının bir belirtisidir. Progesteron içeren tüm örnekler önfaz geçişini ortadan kaldırmıştır.

FTIR spektroskopisinde C=O gerilme modları incelemesi, progesteronun DPPC lipozomlarının ara bölgesi ile hidrojen bağı yapmadığını, bunun yerine sistemde serbest karbonil grupları oluşturduğunu göstermiştir. Progesteronun katılımıyla ester gruplarının düzensizleştiği ve bu etkinin 6 ve 9 mol% konsantrasyon değerleri için belirgin olduğu bulunmuştur.

Lipozom kafa gruplarının 3mol% progesteron bulunurken her iki fazda, 6mol% progesteron bulunurken sıvı kristal fazda hidrojen bağı yaptığı PO_2^- gerilme modunun kızılötesi spektroskopisi ile gözlenmiştir. Hidrojen bağı ya progesteronun hidroksil grubu ile ya da kafa grubu etrafında bulunan su molekülleri ile yapılmıştır. Progesteronun diğer konsantrasyonları ile, hidrojen bağ yapımına ilişkin kanıt bulunamamıştır.

Anahtar kelimeler: DPPC lipozomlar, Progesteron, FTIR, Törbiditi, DSC.

ACKNOWLEDGMENTS

TABLE OF CONTENTS

xiii

LIST OF TABLES

LIST OF FIGURES

xvii

CHAPTER 1

INTRODUCTION

1.1 General Introduction

Membranes perform many functions. They isolate cells and their organelles physically and chemically from their environment. They also house a variety of channels, carriers, and pumps to control the transport between the cell and its environment. Transport properties are controlled by several classes of physicochemical variables and are modulated by signalling molecules such as hormones.

The classically-accepted mechanism of steroid hormone action involves their binding to specific intracellular receptors, initiating gene transcription and protein synthesis (Beato, 1989). However, some steroid actions are non-genomic; they insert themselves into the bilayer of target cell plasma membranes, potentially altering the fluidity and function of the membrane.

Progesterone, which is one of the steroid hormones, is secreted by the corpus luteum. It has a planar configuration permitting insertion into membranes. Because of its chemical and physical properties and abundance in the tissue, progesterone

plays a structural functional role in the membranes of a luteal cell. It controls the functions of female reproductive organs. Progesterone also actively participates in the regulation of blood pressure and other cardiovascular regulations (Rylance et al., 1985 and Regensteiner et al., 1991). Progesterone is used as a drug in the treatment of osteoporosis (Leonetti et al., 1999), hypertension (Regensteiner et al., 1991) and endometrial cancer (Persson et al., 1989).

Liposomes enable performing controlled studies. Their composition and size can be controlled with the type of liposome chosen and the method it is prepared. Phosphatidylcholine (PC) is the predominant phospholipid found in natural membranes. The permanent positive charge on the choline of the headgroup counteracts the negative charge on the phosphate to give a neutral, very hydrophilic headgroup.

The purpose of this study is to investigate the location of progesterone in the model membrane; its effect on the main and pre-transition profile, order and dynamics with respect to its interaction with membrane headgroup and acyl chain with different progesterone to lipid ratios for a temperature range of $25\text{-}70^{0}C$ by using different non-perturbing biophysical techniques; namely, Fourier Transform Infrared (FTIR) spectroscopy, turbidity at 440 nm and Differential Scanning Calorimetry (DSC).

In the first chapter, information about the structure and function of membranes will be presented in detail. Since progesterone is a steroid hormone,

information about steroid hormones will be given. Basic principles underlying the spectroscopic techniques used in this study will be explained. The theory of Fourier Transform will be discussed. In the remaining chapters, the results of this study will be presented.

1.2 Membranes

1.2.1 Biological Membranes

Every cell is surrounded by a cell membrane. It is also called plasma membrane. Membranes define the boundary of the cell and its organelles, and controls communication between the exterior and interior. In all cells, the plasma membrane has several essential functions. These include transporting nutrients into and metabolic wastes out of the cell; preventing unwanted materials in the extracellular environment from entering the cell; preventing loss of needed metabolites and maintaining the proper ionic composition, pH ($\approx$ 7.2), and osmotic pressure of the cytosol. To carry out these functions, the plasma membrane contains specific transport proteins that permit the passage of certain small molecules but not others. The transport mechanisms are also related with the fluidity of the membrane.

1.2.1.1 Structure of the Membrane

The history of modelling the membrane structure begins with the widely accepted Davson- Danielli model, proposed in 1935, which portrayed the membrane as a sandwich: a phospholipid bilayer between two layers of globular protein (Fig.1.2.1.1.1). However, in 1972, S. Singer and G. Nicolson proposed that the globular proteins are inserted into the lipid bilayer, with their nonpolar segments in

3

contact with the nonpolar interior of the bilayer and their polar portions protruding out from the membrane surface. In this model, called the fluid mosaic model, a mosaic of proteins float in the fluid lipid bilayer (Fig.1.2.1.1.2).
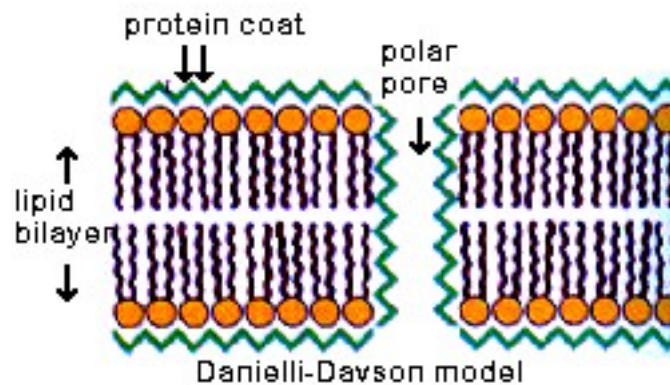
Figure 1.2.1.1.1. Shematic illustration of Danielli-Davson model of membrane
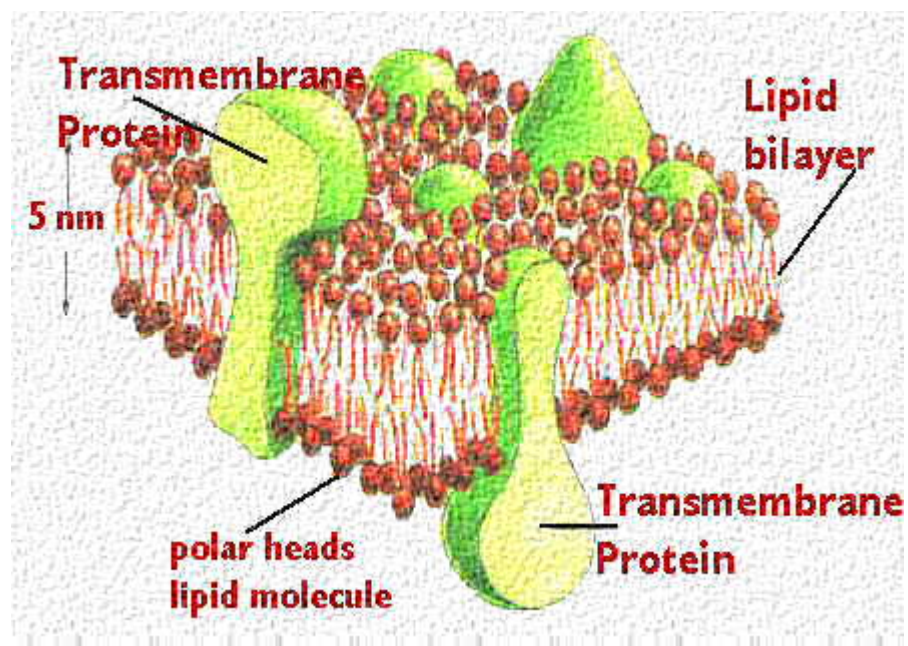
Figure 1.2.1.1.2. Shematic illustration of fluid mosaic model of membrane

Membranes consist mostly of protein and lipid. Depending on the origin of the cell, lipids contribute from 20% to 80% of the weight of the membrane. The lipid layer that forms the foundation of a cell membrane is composed of molecules called phospholipids. A phospholipid has a backbone derived from a three-carbon molecule called glycerol (Figure 1.2.2.3). Attached to this backbone are fatty acids, long chains of carbon atoms ending in a carboxyl (-COOH) group. A phospholipid has two fatty acid chains attached to its backbone. The third carbon on the backbone is attached instead to a highly polar organic alcohol that readily forms hydrogen bonds with water. Since this alcohol is attached by a phosphate group, the molecule is called a phospholipid.

One end of a phospholipid molecule is strongly nonpolar (water-insoluble), while the other end is strongly polar (water-soluble). In Figure 1.2.1.1.3 shown below, one of the nonpolar tails is the straight chain fatty acid (saturated) and the other tail has a cis-double bond (unsaturated). This cis bond influences packing and movement in the lateral plane of the membrane.
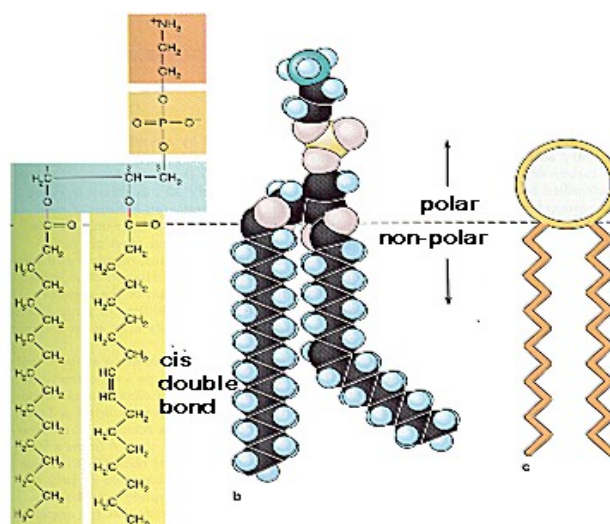
Figure 1.2.1.1.3. Three different ways of illustrating a phospholipid molecule, showing polar head group and nonpolar tail with a double-cis bond.

When a group of phospholipid molecules are placed in water, the polar water molecules repel the long nonpolar tails of the phospholipids. The nonpolar tails of the end up packed closely together by van der Waals bonds, sequestered away from water. Every phospholipid molecule orients to face its polar head toward water and its nonpolar tails away. When two layers come together with the tails facing each other, the resulting structure is called a lipid *bilayer*. Lipid bilayers form spontaneously, driven by the tendency of water molecules to form the maximum number of hydrogen bonds. The nonpolar interior of a lipid bilayer impedes the passage of any water-soluble substances through the bilayer, which is the key biological property of the lipid. Due to the cis bond in one of the tails of the phospholipid, they can not be tightly packed and it makes the bilayer difficult to freeze. The lipid bilayer gives the membrane its fluidity.

1.2.2 Liposomes

The term "liposome" can be defined as any lipid bilayer structure, which encloses a volume. Since they mimic real biological membranes, they are studied to understand the physical and biochemical properties of biomembranes. When the liposomes are inserted in aqueous media, they form bilayers which are generally spherical and contain multiple bilayers forming concentric shells. These liposomes are termed multilamellar vesicles or MLV. There are also single-walled or unilamellar vesicles which can have different sizes. Small unilamellar vesicles (SUV) have diameters in the range 100 Å to 500 Å. Very large or cell-sized phospholipid vesicles can also be prepared and used as model membranes, with diameters as large as 300 μm (Mueller et al., 1983). Real biological membranes are in the form of unilamellar liposomes of approximately 10^5 Å in diameter.

The primary use of liposomes is as model membranes, in which proteins or drugs are incorporated and studied. In small unilamellar vesicles (SUV), although the population homogeneity is advantageous, the small size can be a disadvantage. The small radius of curvature of SUVs results in packing difficulties of lipids. The surface area of the outer monolayer of lipids is almost twice that of the inner monolayer, and about 70% of the lipids on SUVs are in the outer leaflet. This packing phenomenon is sometimes responsible for the asymmetric orientation of some membrane proteins and drugs reconstituted in vesicle. The thermotropic phase transition of SUVs is broadened (Lentz et al., 1976) presumably as a result of the effect of the small radius of curvature on the transition cooperativity. Phosphatidylcholine and sphingomyelin are examples of SUVs. The most studied

lipid is diphalmitoylphosphatidylcholine (DPPC), which is a neutral lipid and gives spherical vesicles.

1.2.3 Molecular Motions in Bilayers

Membrane dynamics is studied because of its relevance to biological function. Mainly there are two kinds of lipid motion in membranes. Either a part of the molecule moves with respect to another part or the whole molecule moves (Andreoli et al., 1986). The latter kind of motion is named as intramolecular movements and it has four types, namely; lateral diffusion, transverse diffusion or flip-flop, axial rotation, and interchain motions (Fig. 1.2.3.1).
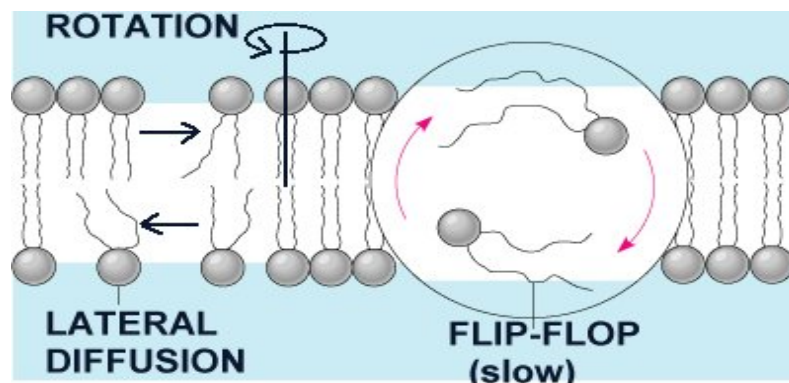
Figure 1.2.3.1. Phospholipid mobility. The types of movement possible for phospholipid molecules in a lipid bilayer.

The lipids of hydrated bilayers in the liquid crystal state diffuse laterally. It is the movement of lipids in the plane of bilayer. A lipid molecule can traverse a distance of 10^5 Å, a typical cell diameter, in about 20 seconds; in other words the

rate of motion is extremely rapid (Fig.1.2.3.2). Diffusion depends on the lipid head group, the chain length, the presence of proteins or other molecules in the bilayer, the ions in the ambient solution and the temperature.

In transverse diffusion or in flip-flop, the lipid molecules rarely migrate from one monolayer to the next. The rate of motion is 10^9 times slower than the lateral diffusion (Fig.1.2.3.2). It takes approximately 12-24 hours for half the phospholipid to exchange into the opposite leaflet. This slow rate is due to large activation energy barrier to movement of polar head group through hydrophobic interior (Smith et al., 1983).

In axial rotation, lipids rotate about their own vertical (long) axis. The rate of motion is again quite fast (Fig.1.2.3.2).

Interchain motions are due to kinks and flexing in the acyl chain of phospholipids. There is free rotation about each C-C bond, with minimum energy preference. The *trans* configuration is the most stable formation for acyl chain. *Gauche* is a configuration that is formed by 120^0 rotations about C-C bonds and they are designated as g^+ and g^- depending on the sense of rotation in going from one C atom to another (Fig.1.2.3.3). The all-trans configuration allows the chain be maximally extended, whereas a gauche bond alters the direction of the chain.

9
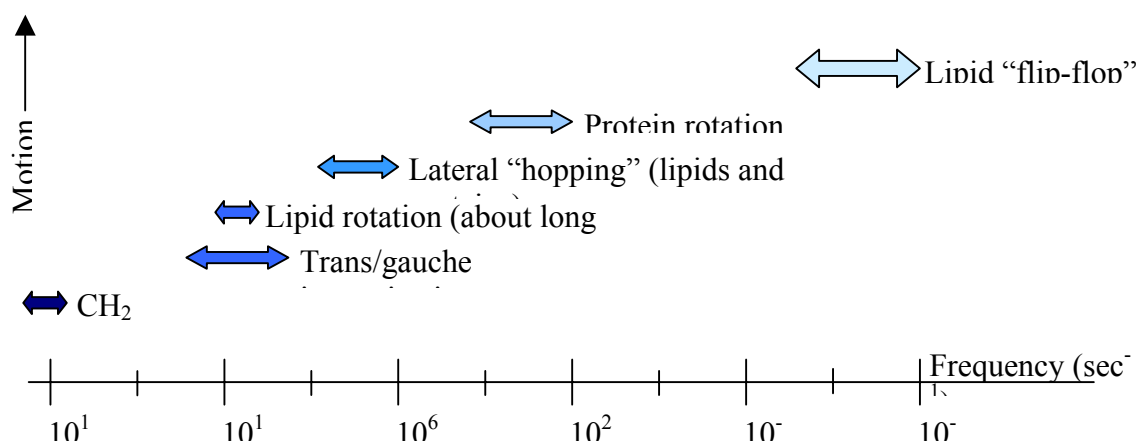
Figure 1.2.3.2. Characteristic frequencies of molecular motions of membrane proteins and lipids. The characteristic times are obtained by taking the reciprocal of the indicated frequencies.
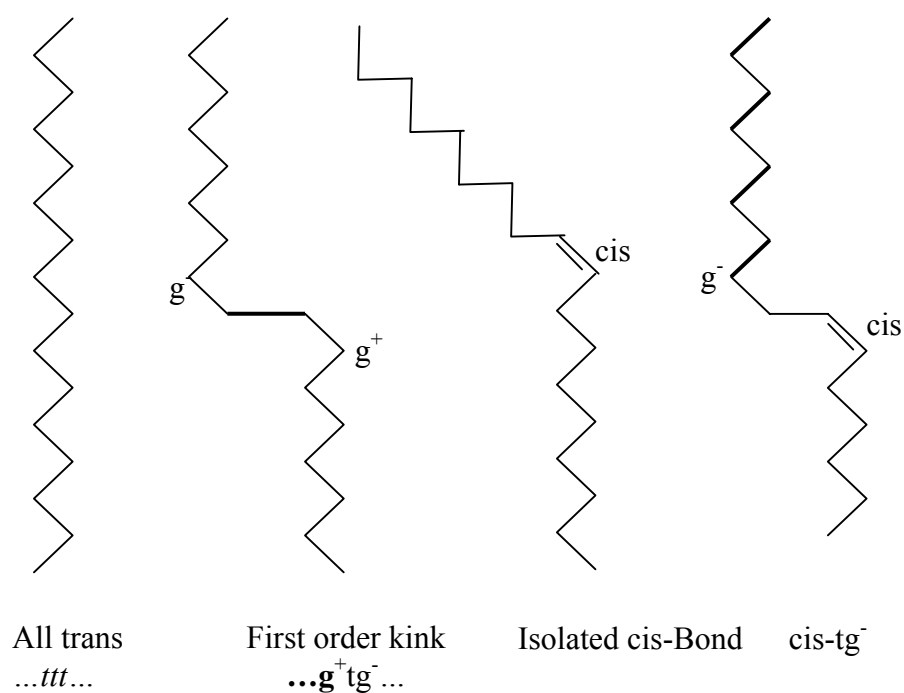
Figure 1.2.3.3. Illustration of various acyl chain configurations.

10

1.2.4 Factors Affecting the Physical Properties of a Membrane

1.2.4.1 Heat

Phospholipids undergo an endothermic, liquid crystal ↔ solid (or gel) phase transition at a particular temperature called phase transition temperature (T_t). In the packing of lipid molecules, defects or vacancies are present in the solid bilayer. The defect is a display of natural entropy or in other words disorder. The occurrence of defects increases with increasing temperature. At the transition temperature, the defects are the sites of initial melting of the lipid molecules forming small groups of fluid lipid molecules. At the transition state, three coexisting lipid phases are encountered: the gel phase, the liquid crystalline phase and interfacial lipid phase. The interfacial lipid phase is the layer of lipid molecules in between the solid and liquid crystalline phases. As the temperature is further increased, the remaining solid domains rapidly melt into an all fluid phase.

The T_t is characteristic for each lipid. The liquid crystalline form of the lipids are called L_α, while the solid form is called L_β in which the molecules are arranged in quasi-hexagonal arrays in the plane of the bilayer, with the hydrocarbon chains in all-trans configuration.

Phospholipids like phosphatidylcholine and phosphatidylglycerol show pretransition, which is a transition before the main order-disorder transition event. It covers a rather broad temperature range and involves a small energy change. Experiments performed with phosphatidylcholine bilayer (Janiak et. al, 1976) show an alteration in the long-range order of the lipids in the solid phase during

pretransition. Therefore the bilayers happen to get into rippled structure (P_β').
Formation of this structure depends on a cooperative change in lipid headgroup
orientation.

Lipids assume a liquid crystalline structure above the transition
temperature. The alkane chains become highly flexible near the middle of the
bilayer due to rotational motions about C-C bonds. If the rotation is 1200, it leads
to transient gauche isomer (or kink) formation. As going to methyl end of alkane
chains, the possibility of kink formation increases. This formation leads to
shortening of the bilayer thickness by 0,7 nm on average.

1.2.4.2 Some Characteristics of Amphiphiles

The presence of double bonds, especially the cis-double bond interferes
with the all-trans packing of hydrocarbon chains in the solid phase (Fig.1.2.4.2.1).
The cis double bond keeps the membrane fluid by interfering with the packing
process, until a lower T_t than that of the saturated analogue is reached. As the
number of double bonds increases, T_t decreases. The position of the cis-double
bond in the hydrocarbon chain may also affect the T_t. Moreover, the distribution
of the double bonds between the two hydrocarbon chains is more effective than
having them in one chain.

12
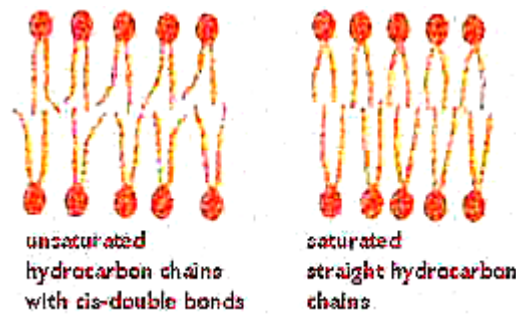
Figure 1.2.4.2.1. Shematic view of saturated and unsaturated hydrocarbon chains.

The charge carried by the phospholipid headgroups can affect lipid fluidity. Phospholipids having negatively charged headgroups melt at lower temperatures than those having uncharged. The conformation of the phospholipid headgroup is also important. Due to the bulky headgroup of phosphatidylcholine, it has a lower T_t than it would have with a smaller headgroup.

One of the main constituents of animal cell membrane is cholesterol, which is a sterol in structure. Presence of it in phospholipid bilayer results in reduced mobility due to the interaction of sterol ring of cholesterol with methylene groups of the phospholipid hydrocarbon chains. Cholesterol fluidises the bilayer below T_t but it has an opposite effect above T_t.

The T_t and phase behaviours differ among the various phospholipid types but all depend strongly on the degree of hydration. The transition temperature decreases as water is taken up by the bilayer. The water molecules bind to the phospholipid headgroups and depress the T_t by approximately 40^0C per water molecule. The

13

bilayers reach a limiting hydration at approximately 30% water. Beyond this limit, the T_t remains constant and further water is not incorporated between the layers.

1.2.5 Order and Disorder

The formally rigid all-trans chains in crystalline phospholipids have a measure of vibrational freedom that increases toward the methyl group tail of the chain. In liquid crystal phases the chains are disordered; any given segment rapidly changing its orientation. It is expected that the motion of a given segment to be more limited near the tightly packed head groups than at the tail ends of the chains but since the orientation of a given segment is time-dependent and unpredictable, only statistical statements can be made about the motion.

Certain molecules can exist in phases that are liquid in the sense that the material flows but crystalline in the sense that the sample has anisotropic physical properties. Conventional liquids are isotropic. Biological membranes are smectic liquid crystals. In this phase the centres of the molecules are arranged in parallel planes, but not necessarily in a definite pattern within the plane. A degree of orientational order exists in smectic phases, and indeed in all liquid crystals. The molecules have two-dimensional translational freedom. This freedom exists for bilayers in the liquid crystal state. Molecules in the smectic phase also have a degree of rotational freedom.

For rod-shaped molecules rotations about the long axis are practically unhindered and have frequencies falling in the range of 10^7 to 10^{10} Hz so that the

molecule has effective axial symmetry. Complete rotations perpendicular to the long axis are strongly discouraged since the molecules get in each other's way. Nevertheless, the long axes of rigid rod-like molecules in liquid crystals fluctuate over a range of angles determined largely by the available space. These fluctuations affect macroscopic and microscopic physical properties of the liquid crystals, measurement of which has allowed quantitative estimates to be made of the degree of angular disorder of the molecules. The results are usually expressed in terms of order parameters.

To define the order parameter, a Cartesian coordinate axis is defined as in Figure1.2.5.1, in which objects in cylindrical shape represent the molecules in smectic phase. The unit vector z′ is defined along the long axis of the molecule so that the movement of the molecules has cylindrical symmetry about this axis, which is called *director*.
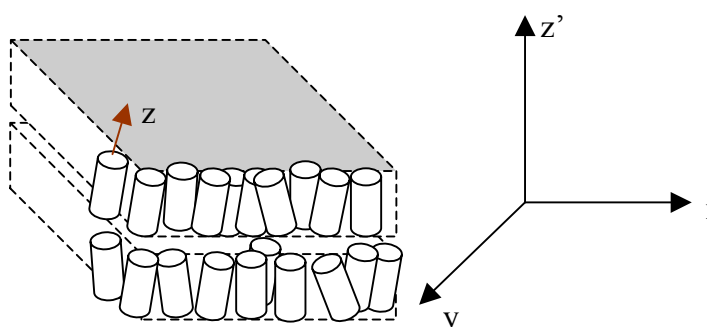
Figure 1.2.5.1. Orientation of molecules in smectic liquid crystals. The molecules are arranged in sheets but their positions are not ordered two-dimensionally within the sheet. Directions of the molecules fluctuate about the normal to the sheet.

The set of order parameters are defined by the equations:

$$S_{ii} = \frac{1}{2}\left(3\overline{Cos^2\theta_i} - 1\right) \quad i = 1, 2, 3 \quad x, y, z \tag{1.2.5.1}$$

where θ_i is the instantaneous angle between the molecular Cartesian coordinate I and the director z′. This angle varies with time due to fluctuations and $\overline{\cos^2\theta_i}$ is a time average for one molecule. Some general properties of S_{ii} can be listed as follows:

a) If the molecule is permanently aligned along the director, then θ_3 is zero and S_{33} = 1, its maximum possible value. Also $S_{11} = S_{22} = -1/2$.

b) Because, by the orthogonality relation between cosines, $\Sigma \cos^2\theta_i = 1$, it follows that $\Sigma S_{ii} = 0$

c) In performing the average in the equation for S_{ii}, θ is allowed to vary from 0 to π. This domain is sufficient to cover all possible orientations of the z-axis because we have assumed that the movement of the molecule is cylindrically symmetric about the director.

d) It is commonly assumed that $S_{11} = S_{22}$ that is, $S_{xx} = S_{yy}$. This implies either that the molecule has cylindrical symmetry about its z-axis or that it rotates about that axis in a time short compared with the time scale of the experiment.

e) For a molecule undergoing isotropic tumbling, S_{33} = 0. This result can be obtained by noting that θ_3 ranges over all angles between 0 and π but the probability of θ_3 falling in the interval θ_3 to $\theta_3 + d\theta_3$ is given by $Sin\theta_3 d\theta_3$. Then

$$S_{33} = \frac{1}{2}\left(3\overline{\cos^2 \theta_3} - 1\right) = \frac{1}{2}\left(3\int_0^\pi \cos^2 \theta \sin \theta d\theta - 1\right) = \frac{1}{2}\frac{\left(-\cos^3 \theta\right)_0^\pi}{\left(-\cos \theta\right)_0^\pi} - 1 = 0 \qquad (1.2.5.2)$$

Since $\Sigma S_{ii} = 0$ and we are assuming that $S_{11} = S_{22}$, it follows that S_{11} and S_{22} are also zero.

f) The definition of order parameters is operational. Two techniques give different answers if they have different time scales.

In the crystalline phase the hydrocarbon chains of phospholipids are rigidly ordered, apart from thermal vibrations. In this phase, the chains have limited freedom of motion, and it is possible to concentrate selectively on individual segments in the chains and determine their order parameters. The measurement of order depends on the anisotropy of the spectra of molecular fragments.

1.2.6 Forces within Macromolecules

The strongest interactions within biological molecules are covalent, i.e., the bonding that completes electron shells. However, there are also noncovalent bonds. One type of the noncovalent bonds is electrostatic (ionic) bond, which occurs between two charged, or partially charged, groups within the interior of a macromolecule. Coulomb's law gives the force between two charges as

$$F = \frac{1}{4\pi\varepsilon_0}\frac{q_1 \cdot q_2}{r^2} \qquad (1.2.6.1)$$

17

where ε_0 is the permittivity constant of the medium between two charges q_1 and q_2, and r is the separation distance between the charges. If the medium between the charges primarily is water, the interactions are significantly weakened. This is because water forms a good dielectric medium. Dielectric materials have permanent dipole moment, which masks the electrostatic interactions between charges. This property of materials is shown by a unitless constant κ. The dielectric constant of bulk water at 20^0C is $\kappa = 80$, which implies that the energies associated with electrostatic interactions in aqueous media are approximately 100 times smaller than the energies of covalent association. However, it is conceptually difficult to determine the dielectric constant within the interior of a molecule. Electrostatic interactions between two charged particles are the strongest noncovalent forces. Weaker electrostatic interactions occur between dipoles and ions.

Although a water molecule is electrically neutral as a whole, electrons are asymmetrically distributed within the molecule. The oxygen atom tends to draw electrons away from the hydrogen nuclei, leaving the latter with a small net positive charge. This positive and the excess negative charges about the oxygen nucleus give the molecule a dipolar character. Several water molecules thus can interact through weak associations called hydration force between the electronegative oxygen nuclei and electropositive hydrogens on neighbouring molecules. Such interactions, which arise because the electrons on one molecule can be partially shared with hydrogens on another, are known as hydrogen bonds. Hydrogen bonds constitute weak interactions and they can be broken easily.

Transient fluctuations in the distribution of electronic charge within molecules or groups of molecules result in weak noncovalent interactions and are known as van der Waals forces. They can be either attractive or repulsive. Both the electron and the nuclear charge distribution in a molecule continually fluctuates at the demand of the uncertainty principle and thermal excitation. At any given moment, even a nonpolar molecule is almost certain to have a finite dipole moment. The origin of van der Waals force is that the fluctuations in the dipoles of different molecules are not independent. The time-varying dipole of a given molecule produces a time-varying electromagnetic field at the position of the second molecule, which adjusts its own fluctuations to those of the field in such a way as to lower the energy of interaction of its dipole with the field. In the case of two static dipoles, provided they are free to orient themselves, their interaction is always finally attractive. Repulsive van der Waals force arises when non-covalently-bonded atoms or molecules come too close together.

All of the forces mentioned above are inversely proportional with the separation distance between the molecules. A comparison of the degree of this proportionality with the type of force is given in Table 1.2.6.1.

Table 1.2.6.1. Range of some intermolecular interactions expressed as the power of the intermolecular separation.

Range of Interaction	Type of Interaction
1 / R	Charge-charge
1 / R^2	Charge-dipole
1 / R^3	Dipole-dipole
1 / R^6	Van der Waals (dipole-induced dipole)
1 / R^{12}	Van der Waals repulsive forces

Internal potential energy of a molecule, when all the forces mentioned above are considered, is written as

$$V(r) = \Sigma k_b (b - b_0)^2 + \Sigma k_\theta (\theta - \theta_0)^2 + \Sigma \left[\left| k_\phi \right| - k_\phi \cos n\phi \right] + \Sigma k_w (w - w_0)^2$$
$$+ \Sigma \frac{q_i q_j}{r_{ij}} + \Sigma \left(\frac{A_{ij}}{r_{ij}^{12}} - \frac{B_{ij}}{r_{ij}^6} \right) + \Sigma \left[\left(\frac{A}{r_{DA}^\alpha} - \frac{B}{r_{DA}^6} \right) \cos^m (\theta_{H.A.AA}) \right] \quad (1.2.6.2)$$

The first term represents the stretching of bonds between the molecules, where k_b is a constant and the term in parenthesis represents the difference between instantaneous and equilibrium bond length. The second term in eqn. 1.2.6.2 is the bond angle energy due to bending, which depends on the difference between the instantaneous and equilibrium values of the bond angle θ. The third term in equation signifies torsional potential energy for chain molecules such as lipids and here, ϕ is the angle of torsion. The fourth term is due to the Coulombic interaction between the neighbouring atoms, where k is a constant and w is the frequency of oscillation. The

fifth term pertains to electrostatic interactions between pairs of atomic nuclei, where q is the charge and r is the distance between the atoms. The sixth accounts for van der Waals interactions, where A and B are constants and their values are determined by the sizes of the atoms, and r is the separation distance between centres of atoms. The last term signifies hydrogen-bond energies, where A and B are constants, r is the distance between the atoms.

1.3. Steroids

1.3.1. Structure of Steroids

Steroids are a group of plant and animal lipids that have the tetracyclic ring system shown in figure below. Steroid hormones are crucial substances for the proper function of the body. They mediate a wide variety of vital physiological functions ranging from anti-inflammatory agents to regulating events during pregnancy. They are synthesized and secreted into the bloodstream by endocrine glands such as the adrenal cortex and the gonads (ovary and testis). The properties common to the tetracyclic ring system of most naturally occurring steroids are;

1. The fusing of rings is trans and each atom or group at a ring junction is axial.

2. The pattern of atoms or groups along the points of ring fusion is nearly always trans-anti-trans-anti-trans.

3. Because of this arrangement of atoms or groups along the points of ring fusion, the tetracyclic steroid ring system is nearly flat and quite rigid.

4. Many steroids have axial methyl groups at C-10 and C-13 of the tetracyclic ring system (Fig.1.3.1.1).
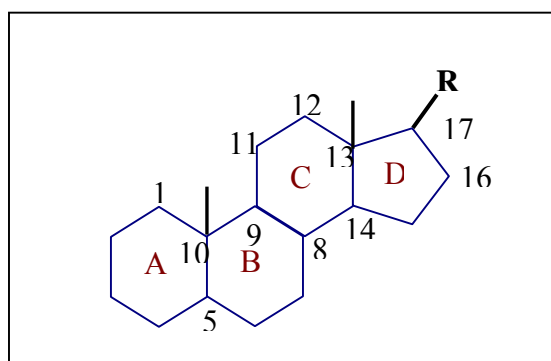
Figure 1.3.1.1. Schematic representation of basic structure of steroids. "R" represents the various side chains. Numbers indicate the custom representation of numbering of carbon atoms.

1.3.2. Steroid Hormones

Steroid hormones are synthesized from cholesterol, which is also a steroid in structure, in the smooth endoplasmic reticulum. They are lipophilic and they can not be stored in vesicles from which they would diffuse easily. Due to their solubility in lipids, steroid hormones are synthesized when needed as precursors. There are five major classes of steroid hormones. They are the progestagens (progestational hormones), glucocorticoids (anti-stressing hormones), mineralcorticoids (Na+ uptake regulators), androgens (male sex hormones), and estrogens (female sex hormones). The structures of some of the hormones are shown in Figure 2. With the exception of retinoic acid, the steroid hormones are all derived from cholesterol. Steroids with 21 carbon atoms are known systematically as *pregnanes*, whereas those containing 19 and 18 carbon atoms are known as *androstanes* and *estranes*, respectively.

Steroids can act through two basic mechanisms: genomic and non-genomic (Brann et al., 1995). The classical genomic action is mediated by specific

22

intracellular receptors, whereas the primary target for the non-genomic one is the cell membrane. Steroid actions, mediated by cell membrane, include effects on brain (GABA$_A$ receptor, oxytocin receptor, neuronal activity), on intestine (calcium transport, smooth muscle contractions), on uterus (contractions), on sperm (calcium influx, acrosome reaction), and oocyte (maturation). Many clinical symptoms seem to be mediated through the non-genomic route, such as; premenstrual tension, fatigue, decreased immediate recall, anxiety, epilepsia, obstipation, uterine contractions, many symptoms caused by elevated calcium concentrations, circulation problems, part of sexual behavioral responses, postpartum depression and rheumatoid arthritis. Non-genomic action is characterized by rapid effect of short duration. There are three possible mechanisms of non-genomic action: (1) non-specific effect on membrane fluidity caused by lipophilic properties of steroids (2) binding to specific steroid membrane receptors, which, in turn, activate a cascade of second messengers and (3) binding and modulation of neurotransmitter membrane receptor (GABA$_A$) (Tuohimaa et al., 1996).
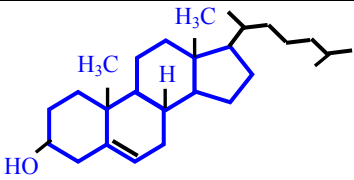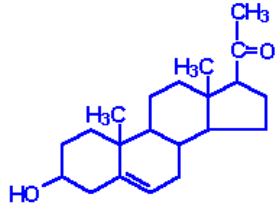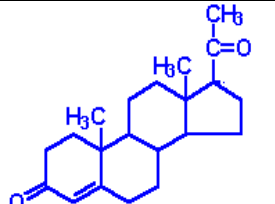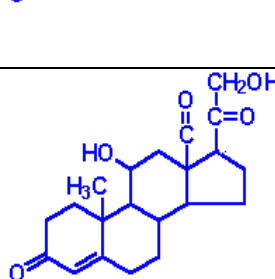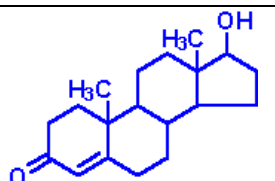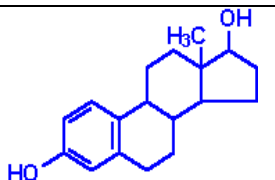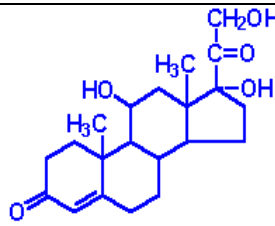
	Cholesterol: parent steroid from which all the steroid hormones are produced
	Pregnenolone: produced directly from cholesterol, the precursor molecule for all C_{18}, C_{19} and C_{21} steroids
	Progesterone: a progestin, produced directly from pregnenolone and secreted from the *corpus luteum*, responsible for changes associated with luteal phase of the menstrual cycle, differentiation factor for mammary glands
	Aldosterone: the principal mineralocorticoid, produced from progesterone in the *zona glomerulosa* of adrenal cortex, raises blood pressure and fluid volume, increases Na^+ uptake
	Testosterone: an androgen, male sex hormone synthesized in the testes, responsible for secondary male sex characteristics, produced from progesterone
	Estradiol: an oestrogen, principal female sex hormone, produced in the ovary, responsible for secondary female sex characteristics
	Cortisol: dominant glucocorticoid in humans, synthesized from progesterone in the *zona fasciculata* of the adrenal cortex, involved in stress adaptation, elevates blood pressure and Na^+ uptake, numerous effects on the immune system

Figure 1.3.2.1. The structure of cholesterol and some steroid hormones from each steroid hormones group.

1.3.2.1. Progestagens

Pregnenolone is an intermediate in the synthesis of all steroid hormones and of progesterone. It is derived from cholesterol by two hydroxylations (two steps), at C20 and C22, followed by cleavage between C20 and C22 as catalysed by the mitochondrial enzyme desmolase. The net result is that six (6) carbons are removed from the C17 sidechain. All three steps require molecular oxygen (O-2) and NADPH (nicotinamide adenine dinucleotide phosphate hormone). Pregnenolone formation is stimulated by the anterior pituitary hormone ACTH (adrenocorticotropic hormone).

1.3.2.1.1. Progesterone

Progesterone is synthesized from cholesterol and acetyl coenzyme A under the control of LH. LH increases the production of cyclic adenosine monophosphate (cAMP), which is formed from adenosine triphosphate (ATP) and is responsible for the intracellular mediation of hormonal effects on various cellular processes (as lipid metabolism, membrane transport, and cell proliferation) (Borgese et al., 1992; Gotteman and Fletschmann, 1986). Increased cAMP level causes the cholesterol to be produced and secreted into the blood in increased amount, which is then transferred to pregnenolone. Pregnenolone is used to synthesize testosterone and progesterone, and all these hormones are used in the production of estrogens. Progesterone, made from pregnenolone, is the primary progestagen. Progesterone is made by the corpus luteum and the placenta from cholesterol by shortening of the side chain and dehydrogenation of the 3β-OH group. The double bond of cholesterol then migrates so as to be in conjunction with the keto group. It is produced mainly during certain phases of menstruation and during pregnancy. Also it is produced in

little amount by adrenal cortex, testis and ovarian follicle because it is necessary in the production of cortisol and aldosterone. It induces development of endometrium and mammary glands, and inhibits the release of LH (Marbaix et al., 1992; Burke et al., 1996; Harness and Anderson, 1977).

In the first half of menstrual cycle, little progesterone (0,9 ng/ml) exists in the blood. In the second half, progesterone level is increased (1,8 ng/ml) (Muneyyirci-Delale et al., 1999). During pregnancy, especially in the fourth month of pregnancy, progesterone is secreted in great amount from placenta. Oestrogen and progesterone is synthesized by adrenal cortex during the whole pregnancy. Therefore progesterone level throughout the pregnancy is very high. Excess secretion or oral intake of progesterone decreases the level of gonadotropin releasing hormone, produced by the hypothalamus, and it prevents the menstrual cycle and the maturation of follicles during pregnancy.

Progesterone is bounded to transcortin (an alpha globulin produced in the liver) or plasma albumin for the transportation in the body. Before entering the target cell, progesterone breaks down its bonds with the transporter. It goes through the cell membrane and binds to receptors special to progesterone in the nucleus of the cell. These receptors are synthesized with oestrogen. Progesterone-receptor pair influences the production of messenger ribonucleic acid (mRNA). mRNA stimulates the formation of proteins and the cell begins its function (Juengel et al., 1995). For example, if the target cell is a nerve cell, anxiety or anger can be stimulated (Gulinello and Smith, 2003).

1.3.2.1.1.1 Biological Effects of Progesterone

Usually, progesterone shows its effect together with oestrogen. Oestrogen increases the effect of progesterone but progesterone has no effect on the action of oestrogen. In other words, for a cell to be stimulated by progesterone, first oestrogen should act on the cell, and then the cell becomes sensitive to progesterone. However, progesterone shows antiestrogenic effect on the target cell by decreasing the production of oestrogen receptors. Furthermore, excess amount of oestrogen and progesterone have opposite (antagonist) effect (Dauvois et al., 1990). Main target organs of progesterone are uterus, breast and brain.

It induces the development of endometrium and mammary glands, and inhibits the release of LH. The biological function of progesterone consists of the regulation of the reproductive organs. In the human it is formed after the rupture of the follicle and among other things it prepares the uterine mucosa for the deposition of the fertilized ovum. Its prime function is to maintain pregnancy but other functions can be listed as follows:

- Acts as a natural diuretic by binding to aldosterone receptors (Pincus, 1943).

- Helps relieve anxiety by decreasing the level of CO_2 in blood (Bitran et al., 1995).

- Raises body temperature (Cagnacci et al., 1997; Babetta et al., 1976).

- Maintains the lining of the uterus for nurturing a fertilized ovum (Reynolds and Redmer, 1992).

- Makes the cervical mucus accessible by sperm (Sauborn et al., 1976).

- Stops ovulation by the other ovary.

- Prevents rejection of the developing baby.

- Allows for full development of the fetus throughout pregnancy.

1.4 Spectroscopy

1.4.1 Electromagnetic Radiation and Matter

The total energy of a molecule is represented as the sum of individual energies due to different motions the molecule is in. In general it is written as

$$E_{total} = E_{transition} + E_{rotation} + E_{vibraion} + E_{electronic} + E_{electron\ spin\ orientation} + E_{nuclear\ spin\ orientation}$$

In a solution, a molecule can translate, rotate and vibrate, and each of these energies is quantized according to the quantum theory (Campbell, 1984). Quantum theory states that, electromagnetic radiation is emitted, propagated, and absorbed in packets, known as light quanta or photons, each of energy

$$E=h\upsilon \qquad\qquad (1.4.1.1)$$

where h is Planck's constant and υ is the frequency of light. Light waves are described by sinusoidally oscillating electric vectors, **E**, and perpendicular magnetic vectors, **B**. Hence, they are called *electromagnetic radiation* (Fig.1.4.1.1).
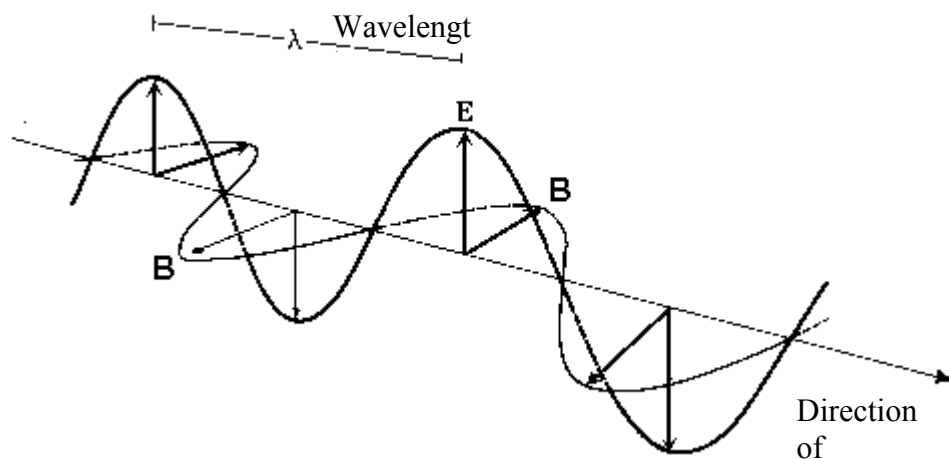
Figure 1.4.1.1. Sketch of electromagnetic radiation.

Photon has the characteristics of both a particle and a wave at the same time, which is known as *wave-particle duality*. When such a photon encounters a molecule, the positive and negative charges in it will be set into forced oscillation at the frequency of the radiation, because they are being constantly pulled apart first one way and then the other by the oscillating electric field of the radiation. This forced motion takes place against the damping forces, which constantly absorb energy. The larger the amplitude of forced motion, the more energy is lost via damping. The maximum amplitude of forced motion occurs at resonance, when the forcing frequency equals the natural oscillation frequency. Hence maximum absorption of radiation occurs at certain specific frequencies, which are the natural oscillation frequencies of electrons in the molecule. This explains the existence of optical absorption spectra and also gives the description of the observed shape of spectral absorption lines. The molecule is said to be *excited* when absorption occurs. An excited molecule can possess any one of a set of quantized energies. The

29

permitted energy values are called the *energy levels* of the molecule. The major
energy levels are determined by the possible spatial distributions of the electrons and
are called electronic energy levels. These levels are further divided into sub-levels
due to the vibration of atoms in the molecule. All these energy levels are described
by an energy-level diagram (Fig.1.4.1.2).
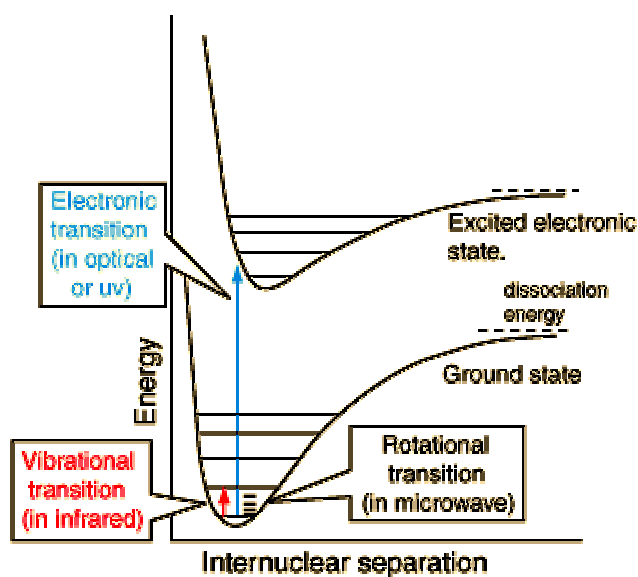
Figure 1.4.1.2. Typical energy- level diagram showing the ground state and the first
excited state. Vibrational levels are shown as horizontal lines and rotational levels
are also shown in between the two vibrational levels in the ground state. A possible
electronic transition between the first vibrational level of the ground state and the
second vibrational level of the first excited state is indicated by the long arrow. A
vibrational transition within the ground state is indicated by the short arrow.

The absorption of energy is most probable only if the amount absorbed corresponds to the difference between energy levels of the atom. This is expressed by stating that light of wavelength λ can be absorbed only if

$$\lambda = \frac{hc}{E_2 - E_1} \qquad (1.4.1.2)$$

in which E_1 is the energy level of the atom before absorption, E_2 is an energy level reached by absorption, and c is the speed of light.

A plot of the probability of absorption versus wavelength is called an *absorption spectrum* and absorption spectroscopy refers to the gathering and analysis of absorption data. If all transitions were in between only the lowest vibrational levels of the ground state and the first excited state, then an absorption spectrum would consist of narrow, discrete lines. However, because transitions are possible from the ground state to any of the vibrational and rotational levels of the first excited state and because the lines have finite width, a spectrum appears to be a relatively smooth curve. There are various factors contributing to the broadening of a line in the spectrum, some of which are listed below:

1. Natural line-width. Quantum mechanics states that for a system that changes with time, it is not possible to define the energy levels exactly. This phenomenon is formulated by one form of the Heisenberg uncertainty principle;

$$\Delta E \; x \; \Delta t \approx h \qquad (1.4.1.3)$$

where ΔE and Δt are the uncertainties in the energy and lifetime of a quantized energy level respectively. If the lifetime of a molecule in an excited state is Δt, then its energy is not exactly E but has a spread of energy ΔE around E. To specify the energy of a state exactly ($\Delta E = 0$) requires that the molecule in that state have an infinitely long lifetime. Since no molecule satisfies this condition, no excited state has a precisely defined energy and that spectral lines have a finite width. This is called lifetime broadening. In the visible spectrum for $\Delta t = 10^{-8}$ sec, a typical lifetime for an excited electronic state, eqn.(1.4.1.3) and (1.4.1.4) give $\Delta \bar{v} = 0,003 cm^{-1}$. Since

$$v = c / \lambda \qquad\qquad (1.4.1.4)$$

$\Delta\lambda = 0,001$ Å which is negligibly small.

2. *Spectrum broadening*. An observed spectrum is broadened because it is the total effect of a large number of molecular transitions, which may be modified by

(a) *Doppler shifts* due to velocity (ϑ) of the molecule in the line of vision, in accordance with the relation:

$$\Delta \bar{v} / \bar{v} = \Delta\lambda / \lambda = \vartheta / c \qquad\qquad (1.4.1.5)$$

This effect is greatest for light molecules, e.g., for H_2 at $300^0 K$, this gives

$\Delta\lambda = 0, 04$ Å, at $\lambda = 6000$ Å

(b) Pressure broadening. The quantized energy levels of a molecule are modified by forces exerted by its neighbors, so that for gases at high pressure, and still more for liquids and solids, the effective width of a spectrum line may be considerably increased.

3. Dissociation. If a molecule becomes dissociated the translational energy of the components formed is naturally unquantized and the associated spectrum is truly continuous.

4. If the lines of a spectrum are so close together that a given spectrometer is unable to resolve them, the spectrum will be apparently continuous.

1.4.2 Infrared Spectroscopy

A change in the energy levels is called a transition. Low-energy transitions between vibrational levels within a single electronic state produce radiation in the infrared region of the electromagnetic spectrum. Fig.1.4.2.1 shows a part of the electromagnetic spectrum including the infrared region. This region includes radiation in wavenumbers between 14000 and 20 cm^{-1}. The spectral range of greatest use is the mid-infrared region, which covers the wavenumber range from 200 to 4000 cm^{-1}. The remaining parts are named as near and far-infrared region.
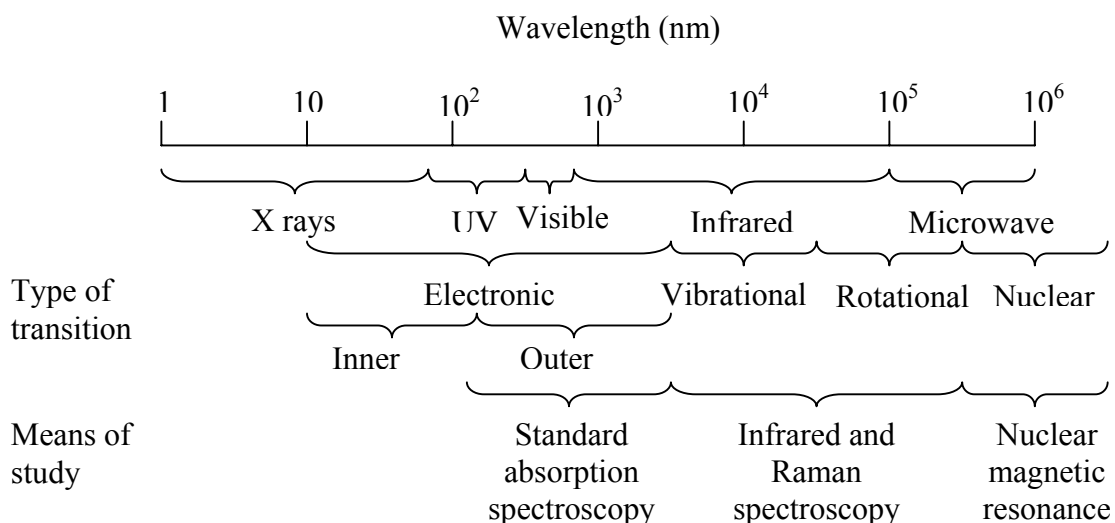
Figure 1.4.2.1. A part of the spectrum which is relevant to physical biochemistry. Characteristic transition types and spectroscopic methods used to investigate these transitions are shown.

Absorption bands occur at almost exactly the same position in compounds of quite different structure, but containing a common molecular group such as the C=O group (Table 1.4.2.1). These group frequencies are described in terms of the motions that the nuclei undergo, being generally classified as twisting, bending, rotating and vibrational (Fig. 1.4.2.2).
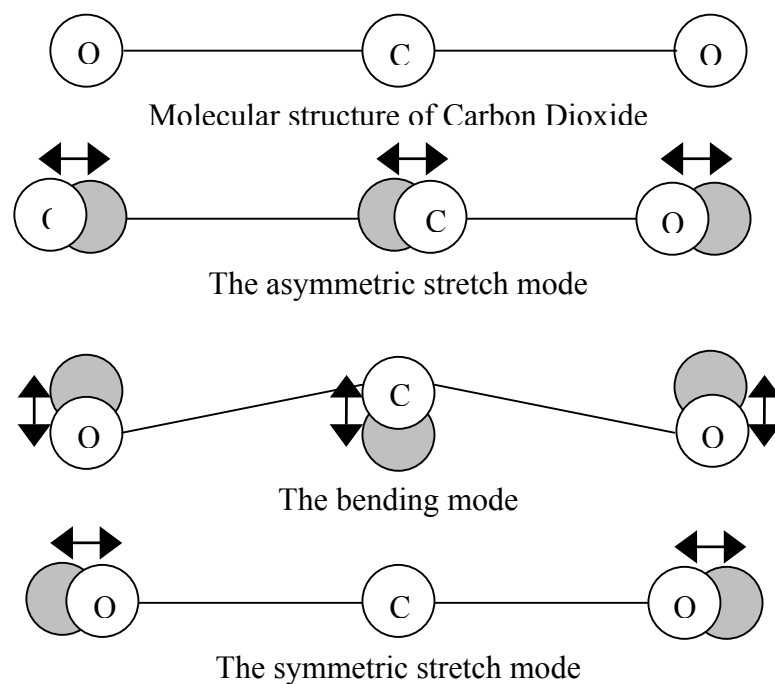
Figure 1.4.2.2. Types of normal vibrations for CO_2 molecule.

The stretching or contracting of a bond is similar to the behaviour of a spring, since there is a restoring force (see Appendix B). The vibrations of the bond can be analyzed in terms of the molecule's undergoing simple harmonic oscillations about its equilibrium bond length. The vibrational frequency, υ_{vib}, is given by

$$\upsilon_{vib} = \frac{1}{2\pi}\sqrt{\frac{k}{\mu}}$$

(1.4.2.1)

where k is the force constant of the bond and μ is the reduced mass of the molecule, which is given by

$$\frac{1}{\mu} = \frac{1}{M_1} + \frac{1}{M_2}$$

(1.4.2.2)

where M_1 and M_2 are the atomic masses of two molecules under consideration.

When a molecule interacts with infrared radiation, some portions of the incident radiation are absorbed at particular wavelengths depending on the chemical structure of the molecule (Table 1.4.2.1). Thus the absorption spectrum of a compound identifies the functional groups comprising the molecule. Infrared spectroscopy is sensitive to changes in chemical structure, conformation and environment that the molecule is in.

An infrared spectrum usually consists of a plot of the absorption of radiation as a function of wavenumber which is sometimes referred to as frequency and is characterized only in terms of the positions of the maxima of each of the absorption bands v_{max} (cm^{-1}).

Table 1.4.2.1. Some characteristic bond wavenumbers in cm^{-1}.

Group	Stretching vibration (cm^{-1}±100cm^{-1})	Group	Bending Vibration (cm^{-1}±100cm^{-1})
≡C−H	3300	≡C−H	700
=C−H	3020	=C⟨H H	1100
>C−H	2960	C − C ≡ C	300
−O−H	3680	≥N−H	1600
−S−H	2570		
≥N−H	3500		
≥C=O	1700		
≥C=N−	1650		
−C≡C−	2050		
>C=C<	1650		
>C−C<	900		
P=O	1250-1300		

1.4.2.1 Instrumentation of Fourier Transform Infrared Spectroscopy (FTIR)

The source of radiation is a heated filament that emits a continuous infrared spectrum. Incoming beam of radiation is directed through a sample cell to a beam splitter, which divides the beam into two. An ideal beamsplitter consists of a non-absorbing film which transmits 50% of the radiation to the mirror, which is moving back and forth over a distance of about 2.5 micrometers at constant speed, whereas 50% of the radiation is reflected to the fixed mirror. Therefore a path difference

37

between the beams is introduced. After being reflected, the two beams will recombine at the detector, which measures the difference in energy between the two beams. A single scan of the entire distance takes about 2 seconds and is stored in the computer. In order that several scans may be added, they must coincide exactly. Obviously, this would be impossible considering the thermal fluctuations and vibrations in the laboratory. In order to solve this problem, a helium-neon laser is simultaneously directed through the Michelson Interferometer and the interference pattern of the laser is used as a frequency reference. A sketch of the interferometer is shown in Fig.1.4.2.1.1.
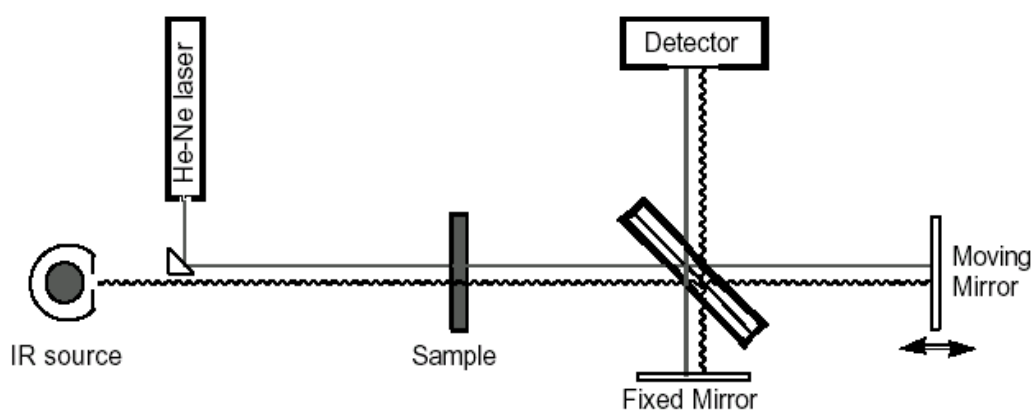
Figure 1.4.2.1.1. Schematic diagram of the optical layout of a Michelson interferometer used in an FTIR Spectrophotometer.

1.4.2.2 Fourier Transform

1.4.2.2.1 The Continuous-Time Fourier Transform

The representation of a continuous and periodic signal in terms of complex exponentials, or equivalently, in terms of cosine and sine waveforms, leads to the Fourier series (see Appendix C). Fourier transform is a method for representing aperiodic signals by decomposing them into a set of weighted exponentials. If *x(t)* is an aperiodic signal, the Fourier transform of it gives;

$$x(t) = \frac{1}{2\pi} \int_{-\infty}^{\infty} X(\omega) \exp[i\omega t] d\omega \qquad (1.4.2.2.1.1)$$

where ω is the frequency of signal and *X(ω)* is;

$$X(\omega) = \int_{-\infty}^{\infty} x(t) \exp[-i\omega t] dt \qquad (1.4.2.2.1.2)$$

$X(\omega)$ is called the Fourier transform of *x(t)*. Thus, $X(\omega)$ is the spectrum of *x(t)* and is a continuous function defined for all values of ω.

Amplitude modulation, multiplexing, filtering, and sampling are among the important applications of the Fourier transform.

1.4.2.2.2 The Discrete-Time Fourier Transform (DFT)

The discrete-time Fourier transform is introduced when the Fourier transform of a function is to be calculated using a digital computer. This type of processor can

handle only numbers and in a quantity limited by the size of its memory. It follows

that the continuous signal *x(t)* should be replaced by a discrete signal *x(n)*. The

discrete-time Fourier transform of the sequence is taken as;

$$X(k) = \sum_{n=0}^{N-1} x(n) \exp\left[-i\frac{2\pi}{N}nk\right] \qquad k = 0, 1, \ldots, \text{M-1} \qquad (1.4.2.2.2.1)$$

where M is the number of frequency samples; Ω is the discrete-time frequency

variable of the signal and is defined as ωT; N is the number of points in time axis of

the signal; and k is defined as;

$$k = \frac{M\Omega_k}{2\pi} \qquad (1.4.2.2.2.2)$$

One of the reasons for the widespread use of the DFT is the existence of

algorithms for their fast and efficient computation on a computer, called fast Fourier

transform (FFT) algorithms.

1.4.2.2.3 Convolution

Let the *x(t)* be the input and *y(t)* be the output signal of a system. From the

definition of delta function *δ(t* , *x(t)* can be written as;

$$x(t) = \int_{-\infty}^{\infty} x(\tau)\delta(t-\tau)d\tau \qquad (1.4.2.2.3.1)$$

The above equation shows that any signal *x(t)* can be expressed as a continuum of weighted impulses. We can also express the output *y(t)* as a linear combination of the responses of the system to shifted impulse signals; that is,

$$y(t) = \int_{-\infty}^{\infty} x(\tau)h(t-\tau)d\tau \qquad (1.4.2.2.3.2)$$

where *h(t - τ)* denotes the response of a linear system to the shifted impulse *δ(t − τ)*. In other words, *h(t - τ)* is the output of the system at time t in response to input *δ(t − τ)* applied at time *τ*. The integral relationship expressed in Equation (1.4.2.2.3.2) is called the convolution integral of signals *x(t)* and *h(t)* and relates the input and output of the system by means of the system impulse response. Since the system under consideration is linear, this type of convolution is also called linear convolution. This operation is represented symbolically as

*y(t) = x(t) * h(t)*   (1.4.2.2.3.3)

If *X(ω)* is the Fourier transform of *x(t)* and if *H(ω)* is the Fourier transform of *h(t)*, then the convolution of two signals can be represented as

$$x(t) * h(t) \leftrightarrow X(\omega)H(\omega) \qquad (1.4.2.2.3.4)$$

Hence, convolution in time domain is equivalent to multiplication in the frequency domain. *H(ω)* is also referred to as the frequency response of the system.

The use of convolution property for linear time-invariant (LTI) systems is demonstrated in Figure (1.4.2.2.3.1).

x(t)	h(t)	y(t) = x(t) * h(t)
X(ω)	LTI	
	H(ω)	Y(ω) = X(ω)H(ω)
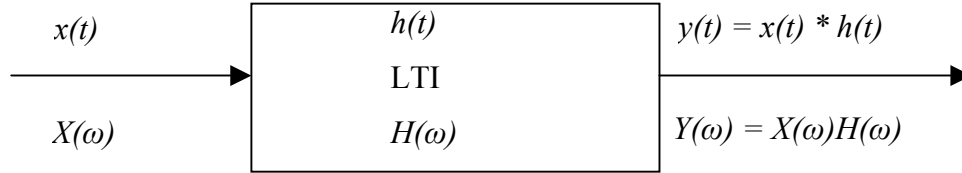
Figure 1.4.2.2.3.1.Convolution property of LTI system response.

For discrete-time systems Equation (1.4.2.2.3.2) is written as

$$y(n) = \sum_{k=-\infty}^{\infty} x(k)h(n-k) \qquad (1.4.2.2.3.5)$$

In certain applications, the convolution of two periodic sequences $x_1(n)$ and $x_2(n)$, with common period N is considered. However, the convolution of two periodic sequences does not converge. In order to solve this problem, we define a different form of convolution for periodic signals, namely, periodic or circular convolution;

$$y_p(n) = \sum_{k=0}^{N-1} x_1(k)x_2(n-k) \qquad (1.4.2.2.3.6)$$

42

In the equation above, $y_p(n)$ comes out to be periodic as well. We denote this operation as

$$y(n) = x_1(n) \otimes x_2(n) \qquad\qquad (1.4.2.2.3.7)$$

Periodic convolution is defined only for sequences with the same period. If the two sequences are not of the same length, we can still define their convolution by augmenting the shorter sequence with zeros to make the two sequences the same length. This is known as zero-padding or zero-augmentation.

1.4.2.2.4 Deconvolution

Deconvolution is the inverse process of the convolution, which is applied when the input signal of a system is to be found with the output and the system response in hand (Fig.1.4.2.2.4.1).
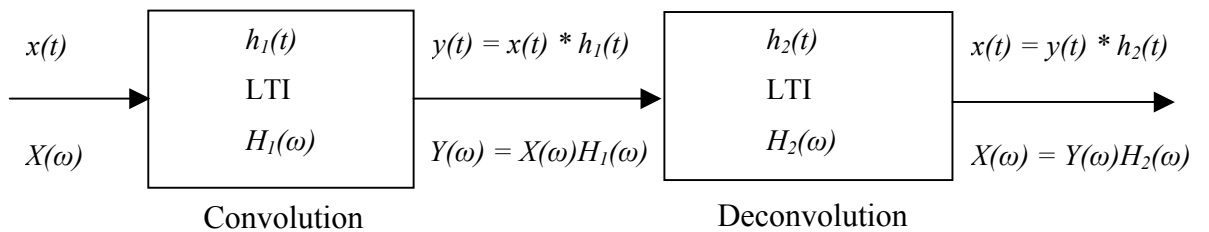
Figure 1.4.2.2.4.1. Convolution and deconvolution property of LTI system response.

Selecting the appropriate filter parameters is critical in obtaining good results with Fourier deconvolution. The deconvolution method used in this study is a special high-pass filter (see Appendix C), which synthetically narrows the effective trace bandwidth features. This aids in identifying the principle bands that comprise a more complex band with overlapping features. This can be useful for more accurate determination of the number of peaks in a trace region, the band positions, and areas.

This application is based on the method described by P.R. Griffiths and G. Pariente (1956). Two filters are employed in this method. An exponential filter is used to sharpen spectral features. In the computer program of FTIR spectrometer, a constant "γ", shown in Equation (1.4.2.2.4.1), is varied by the user to change the shape of this filter. The form of the filter is given by the equation

$$e^{2\pi\gamma X} \hspace{4cm} (1.4.2.2.4.1)$$

where γ is the deconvolution filter constant and **X** is the array (i.e., data file) whose X range is normalized between 0 and 1. This function is multiplied by the Fourier transformed trace, and the data is then reverse Fourier transformed to give the result.

As Fourier deconvolution tends to increase the apparent noise in the data, a low-pass smoothing filter is applied simultaneously. This effectively reduces the noise without loosing peak resolution. The two smoothing filters supported by deconvolve process are the Bessel function and the boxcar function. The Bessel smoothing function (x) is the form;

$$\left[1-\left(\frac{x}{X}\right)^2\right]^2 \hspace{4cm} (1.4.2.2.4.2)$$

where $0 \leq x \leq X$ and X is an array, where the X-axis range is normalized between 0 and 1. Thus, the Bessel filter defines the fraction of the Fourier transformed data to be zeroed and provides a smooth rounding. The boxcar smoothing function simply zeroes points outside the cut-off.

1.4.2.3 Infrared Spectroscopy in Membrane Research

So far, a variety of studies have been made mainly on the organization and dynamics of the lipid matrix. Besides, temperature induced gel to liquid crystal phase transition, which is the total consequence of the changes in the structure or mobility of individual molecular components, is studied by using a variety of spectroscopic techniques such as ESR (Electron Spin Resonance), NMR, Ultraviolet, Raman and Infrared.

Infrared spectroscopy has been applied to the analysis of membrane structure for the last two decades. This technique has several important advantages over conventional methods. The most important of which is the efficient and rapid collection of data. In addition, since a computer is used to obtain the Fourier transform, it is easy to perform many scans to improve the signal-to-noise ratio. Moreover, a temperature controller unit can be connected to the instrument and

hence conformational transitions between the two thermotropic phases of vesicles can be monitored easily.

Studies of biological samples are usually done in aqueous environment. However, water has a high absorbance throughout the infrared region. The main problem is that the concentration of H_2O is 55 molar (mol/liter), while most biologically interesting compounds can be obtained only in the milimolar or less concentration range. Although this poses a severe limitation on the use of infrared, introduction of Fourier transform has partially overcome the problem (Casal and Mantsch, 1984). By Fourier transform, it became possible to remove most of the water absorption bands from the total spectrum. Besides, some experimental techniques have been developed to get rid of the water absorption bands from the spectroscopy. One of which is the usage of heavy water (D_2O) instead of water. This replacement can cause a slight rise, around 0.2 to 0.4^0C, in the phase transition temperature of lipid vesicles. Another method is decreasing the path length of the radiation while going through the sample. In very thin cells, in which the sample is contained, path length varies between 5 and 50 μm. In this way samples are studied in the normal absorption and subtraction of water bands is possible. If the path lengths are greater than 50 μm, radiation can not reach the detector at frequencies corresponding to water absorption bands. Then, subtraction processes become difficult or impossible.

1.4.3 Ultraviolet and Visible Spectroscopy

Electronic spectra involve transitions between different energy levels of the electrons in molecules. Electronic transitions give rise to the interaction of radiation with matter: color, vision, and the conversion of sunlight into energy by plants. The energies involved in these transitions correspond to the absorption of photons in the visible (400-750 nm) and ultraviolet (200-400 nm) regions of the electromagnetic spectrum (Fig.1.4.2.1). The electronic absorption spectra of molecules make it possible to account for their color. The color of a compound is determined by the light that it does not absorb.

The most general application of electronic spectroscopy is to measure concentrations because in most cases there is a direct relationship between the number of molecules present and absorption. In some cases, however, the absorption depends on the molecular environment in a significant way.

The electronic spectrum is usually presented as a plot of absorbance versus the wavelength of irradiation. Two parameters are used to characterize a particular band, its position at the maximum (λ_{max}) and its intensity.

The intensity of light falls off exponentially as it passes through the absorbing sample, which is formulated as;

$$log_{10}\left(\frac{I_0}{I_t}\right) = \varepsilon\,cl \qquad\qquad (1.4.3.1)$$

where I_0 is the radiation incident on the compound; I_t is the transmitted radiation by the compound; ε is the *extinction coefficient,* which is the experimental measure of intensity at a particular wavelength; c is the concentration of the compound; and l is the path length. This equation is also known as the *Beer-Lambert* law. The extinction coefficient is a measure of the absorbing power of the compound and is related to the transition probability at a given wavelength. The variation of ε with wavelength constitutes the absorption spectrum. The absorbance of a compound is represented by A and is given by the Beer-Lambert law (eqn.1.4.3.2). It is also called optical density and is dimensionless. The spectrum can also be presented as absorbance versus wavelength of the compound.

$$A = log_{10}\left(\frac{I_0}{I_t}\right) = \varepsilon\, cl \tag{1.4.3.2}$$

1.4.3.1. Instrumentation of UV-Visible Spectroscopy

Spectrophotometers produce monochromatic light and then accurately measure the light intensity. The major components of a spectrophotometer are the light source, a monochromator, sample holder, a light detector (phototube), and a meter (Fig.1.4.3.1.1). In most instruments a tungsten lamp is used for the visible range and either high pressure H_2 or D_2 lamps are used for UV range. Various devices like a movable prism, a diffraction gradient or filters can generate monochromatic light. Monochromatic light of known intensity is projected through the sample and then measured by a photomultiplier tube. A photomultiplier tube converts the energy of the light photons into electrons. The voltage resulting from

these electrons is measured by a meter and converted to an absorbance value. Spectrophotometers often include accessories such as chart recorders or microprocessors for data analysis.
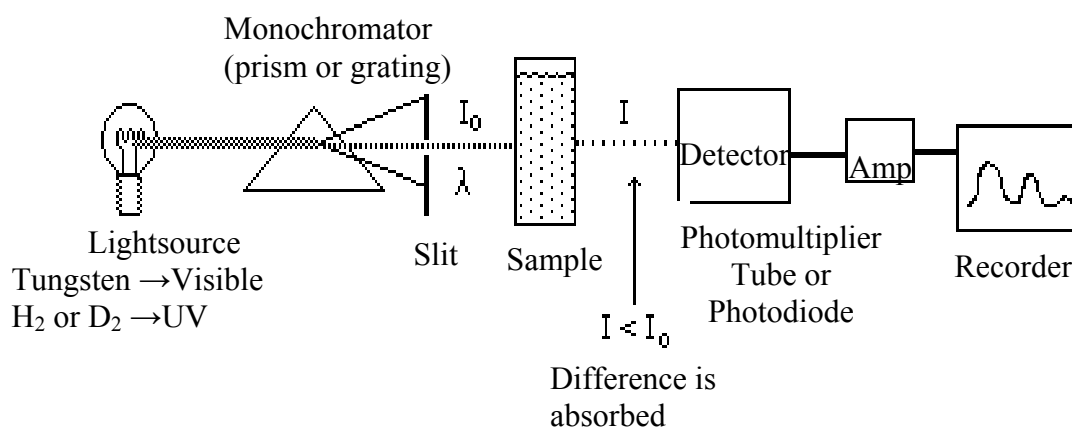
Figure 1.4.3.1.1. Schematic diagram of a single beam spectrophotometer for UV-Visible spectroscopy.

A beam splitter can be placed between the monochromator and the sample; therefore the incoming beam splits into two; one of which passes through the sample and the other passes through a reference. Two rotating mirrors, called choppers, which are synchronized with the displacement of the grating, allow the comparison of transmitted light at the detector of the two beams with the same wavelength. These kind instruments are called *double beam spectrophotometers*.

1.4.3.2 UV-Visible Spectroscopy in Membrane Research

This technique was discovered in 1941 during World War II. US scientists were in a search for a simple and inexpensive technique to find the types of vitamins present in foods, which has vital importance for soldiers. Since then, this spectroscopic method has been applied for many purposes such as the determination of concentration, estimating the structure of a compound, kinetic and thermodynamic studies and enzyme activity.

In membrane research, this technique has been applied to obtain information about the structure and thermotropic phase transition of lipid matrices like FTIR (Severcan et al., 1995). The advantages of this technique are that, only a small amount of sample is required to make the experiment. Rapid collection of data and cheapness of the instrument are other advantages of using UV-Visible spectrometer.

However, there are also limitations. Beer-Lambert Law can not be applied in compounds with high concentration. Concentration effects are not usually encountered at values < 0.01 mole dm^{-3}. Above this value, however, refractive index changes and the perturbing effects of inter-molecular interactions, or of ionic species, on the charge distribution of the absorbing species can affect the value of the absorption coefficient and give rise to either positive or negative deviations. Hence, the sample should be weak in concentration. Also the presence of interfering ions can cause color distortions and invalidate the visual comparison. Furthermore, the solution should not fluoresce and must be homogeneous.

1.4.4 Differential Scanning Calorimetry

Differential scanning calorimetry (DSC) measures the amount of energy (heat) absorbed or released by a sample as it is heated, cooled or held at constant temperature and comparing these values with an inert reference material, such as alumina or just an empty aluminium pan, under similar conditions. DSC also performs precise temperature measurements of phase transitions. In addition, DSC determines the specific heat, heat of fusion, and heat of reaction or heat of polymerization of materials. Since the DSC is at constant pressure, the heat flow rate is equivalent to enthalpy changes:

$$\left(\frac{dq}{dt}\right)_{p} = \frac{dH}{dt} \tag{1.4.4.1}$$

Here dH/dt is the heat flow rate measured in mcal sec^{-1}. The heat flow difference between the sample and the reference is:

$$\Delta\left(\frac{dH}{dt}\right) = \left(\frac{dH}{dt}\right)_{sample} - \left(\frac{dH}{dt}\right)_{reference} \tag{1.4.4.2}$$

and can either be positive or negative. In an endothermic process, such as in most phase transitions, heat is absorbed and, therefore, heat flow to the sample is higher than that to the reference. Hence $\Delta(dH/dt)$ is positive. Other endothermic processes include helix-coil transitions in DNA, protein denaturation, dehydrations, reduction reactions, and some decomposition reactions. In an exothermic process, such as

crystallization, some cross-linking processes, oxidation reactions, and some decomposition reactions, the opposite is true and $\Delta(dH/dt)$ is negative.

A DSC spectrum usually consists of a plot of heat flow as a function of temperature and is characterized in terms of the positions of the maxima or minima of each of the heat absorption bands.

1.4.4.1 Instrumentation of DSC

The calorimeter consists of a sample holder and a reference holder. Both are constructed of platinum to allow high temperature operation. Under each holder there is a resistance heater and a temperature sensor. Currents are applied to the two heaters to increase the temperature at the selected rate. The difference in the power to the two holders, necessary to maintain the holders at the same temperature, is used to calculate $\Delta(dH/dt)$. A schematic diagram of a sample DSC is shown in Figure (1.4.4.1.1). A flow of nitrogen gas is maintained over the samples to create a reproducible and dry atmosphere. The nitrogen atmosphere also eliminates air oxidation of the samples at high temperatures. The sample is sealed into a small aluminum pan. The reference is usually an empty pan and cover.

1.4.4.2 DSC in Membrane Research

DSC is used for investigations of stability and of physical and chemical interactions between the active components of drug (Schneider et al., 1999). Also determination of phase diagrams, characterization of polymers by thermal analysis (John SantaLucia, Jr., 1998), measurement of heat capacity (Cp) for the calculation

of reaction enthalpies from the measured heat capacities of reactants and products, and purity determination of chemicals, chemical half-life determinations (Mayor et al, 2000) and thermal stability and reversibility (Anton et al., 2000) determinations are some of the application areas of the method. In membrane research, thermotropic phase transition from gel to liquid crystalline state is studied by using DSC (Wolf et al., 1990). It gives information about the phase T_t and lipid packing rates in studies of drug-membrane interactions.
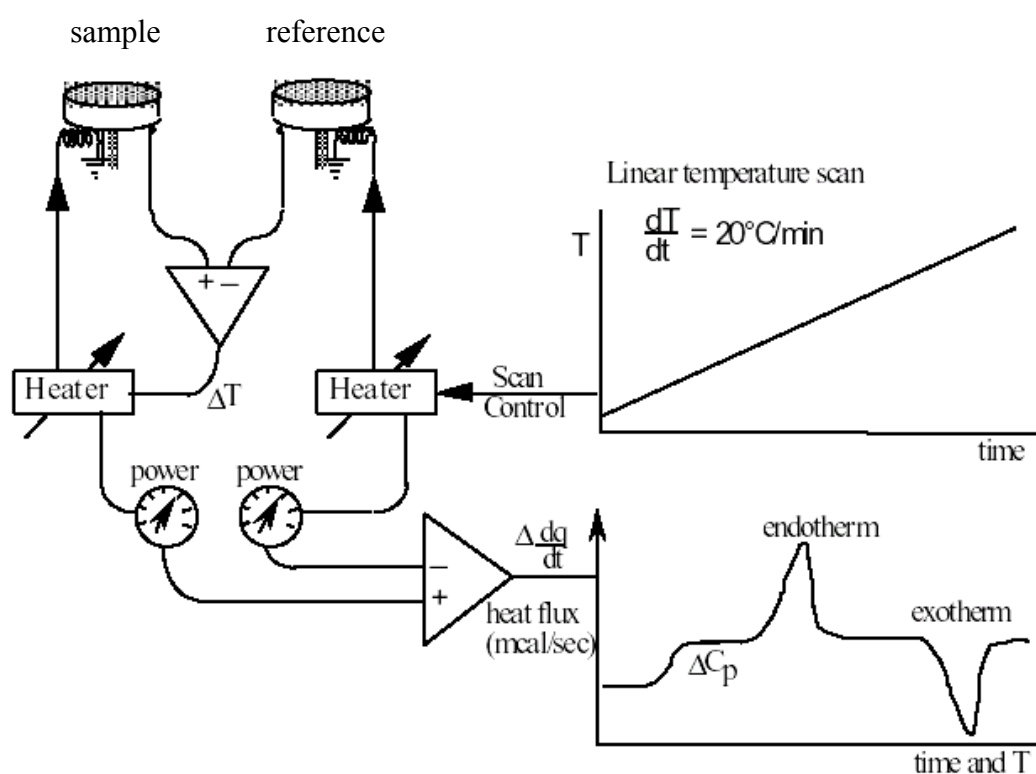
Figure 1.4.4.1.1. Schematic representation of a DSC. The triangles are amplifiers that determine the difference in the two input signals. The sample heater power is adjusted to keep the sample and reference at the same temperature during the scan. A sample plot of enthalpy versus time or temperature graph is also shown.

The main advantage of DSC method lies in the ease and simplicity of operation –in particular both the choice and the rapid change of the required temperatures. This is very important for the investigation of substances with metastable phases. On the other hand there is the disadvantage that it is not possible to carry out experimental manipulations.

As usual, there are some limitations with this method as well. The curve measured when the instrument is empty is called the *zero line*. The shape of the zero line is influenced by the heating rate. Therefore, the heating rate during the calibration of the instrument and actual experiment should be the same. Also the sample should be homogeneous.

The observed peak in the spectrum is affected from a number of conditions such as; the thermal resistance between the sample and temperature sensor (Reichelt and Hemminger, 1983), heating rate, thermal conductivity of the sample, the mass and heat capacity of the sample, and sample purity.

1.5 Literature Review of Progesterone-Membrane Interaction

Jensen et al. in 1968 explained the steroid hormone action as a two-step model, in which steroids diffuse freely across cell membranes and carry out their action at the level of the cell nucleus, where they interact with receptors which then bind DNA. Later in 1978, Baulieu et al. have demonstrated that the progesterone and other steroid molecules are able to promote the maturation of *Xenopus laevis oocytes*

through interaction with cell membrane. It thus appears that, in addition to the receptor-mediated mechanism, steroids also operate through other mechanisms, in particular, through an effect on the plasma membrane. Studies have shown that steroids interact with biomembranes mainly through phospholipids (Sackmann and Trauble, 1972; Sato et al., 1979). Moreover, different steroids act at different levels of the fatty acyl chains in the lipid bilayer (Vincent et al., 1980).

Interaction of progesterone with DPPC multilamellar liposomes was investigated with DSC method by Carlson et al (1983). For a temperature range of $20\text{-}70^0C$, progesterone was studied for concentrations of 5, 10, 20, 30 and 33mol%. It has been found that progesterone eliminates pretransition and broadens the transition peak but changes the enthalpy of transition slightly. It was concluded by a comparison of structures of progesterone and cholesterol that hydroxyl group of progesterone positions near the phospholipid head groups and other parts locate adjacent to the acyl chains. Therefore progesterone is said to associate mainly with the hydrophilic region of synthetic membranes.

The conformations of the A-ring and the 17-acetyl groups of progesterone were examined within DPPC liposomes using nuclear magnetic resonance (NMR) and circular dichroism (CD) in the wavelength regions 260-360 nm (Bueno et al., 1990). Varying concentrations of phospholipids were mixed with 50 μM progesterone. According to the study made in room temperature, progesterone exists in a space of two hydrocarbon chains of one lipid molecule.

Interactions of progesterone with DPPC monolayers were studied at the air/water interface using a tensiometer to measure the change of the monolayer surface tension γ (mN/m) by Dimitrov and Lalchev in 1998. Experiments were carried out at three temperatures: 37 ^{0}C, 41.5 ^{0}C and 47 ^{0}C. 95.9mol% of progesterone lowered the surface tension of monolayer slightly. This effect was explained by the lack of OH group and C-H chain in the structure of progesterone.

Whiting et al. (2000) used phosphatidylcholine liposomes, synaptosomal plasma membranes and sarcoplasmic reticulum to study the interaction of progesterone and membranes. The concentrations of progesterone in phospholipids were 20, 30 and 47mol%. Fluorescence anisotropy measurements at room temperature revealed that lipid fluidity was decreased for all concentrations but no suggestion was made about the location of progesterone in phospholipids.

Another study made to investigate the membrane fluidity effect of progesterone was made by Liang et al. in 2001. Progesterone ranging from 200 nM-20 μM dissolved in 40 mM of phosphatidylcholine was investigated by fluorescence anisotropy and it has been found that progesterone decreased the fluidity of membrane in concentration dependent manner. However, progesterone showed no fluidity effect on HT-hippocampal cell, which was used as plasma membrane.

Fluidity effect of progesterone on erythrocyte membrane was investigated by Electron Paramagnetic Resonance (EPR) technique at 30^{0}C (Tsuda et al., 2002). 10^{-9} M – 10^{-6} M progesterone was dissolved in membrane. It has been shown that

progesterone decreased the order parameter in dose-dependent manner, which means progesterone increases membrane fluidity of erythrocytes.

CHAPTER 2

MATERIALS AND METHODS

2.1 Reagents

Progesterone and dipalmitoyl-L-α-Phosphatidylcholine (DPPC) were purchased from Sigma Chemical Company USA. They were used without further purification.

2.2 Buffer Preparation

Phosphate buffer with neutral pH 7.4 and a concentration of 10 mM was prepared by using Na_2HPO_4 with molecular weight of 141.96 g. 0.2839 g of Na_2HPO_4 powder was added to 200 ml double distilled water and obtained solution was stirred untill the powder was completely dissolved. Either by adding acidic chloride HCl or sodium hydroxide NaOH, pH value was adjusted to 7.4 at room temperature.

2.3 Stock Solution Preparation

Progesterone stock solution was prepared by using progesterone powder of molecular weight 314.5 g. 1 ml ethanol was used to dissolve 5 mg of progesterone.

2.4. FTIR Spectroscopy Study

2.4.1. Preparation of Model Membranes

Multilamellar liposomes were prepared according to the procedure reported by Toyran and Severcan (2002). In order to prepare the liposomes, 5 mg of DPPC was dissolved in 0.15 ml chloroform inside an ependorf to obtain homogeneous vesicles. The solution was then subjected to a stream of nitrogen to remove excess chloroform, which provides uniform distribution of the lipid on the walls of the container. Remaining solvent was removed by subjecting the films to vacuum drying for 2 hours. Thin films were then hydrated by adding 0.025 ml of phosphate buffer. Multilamellar liposomes were formed by vortexing the mixture for 20 min at 20^0C above the T_t of DPPC ($\sim 62^0$C).

In order to prepare progesterone containing liposomes, required amount of stock solution was placed inside the ependorf. Then, the solution in the ependorf was subjected to a stream of nitrogen to remove ethanol and the procedure mentioned above for the preparation of DPPC liposomes was followed.

2.4.2. Sampling for FTIR

Water insoluble CaF_2 quartz windows were used. This kind of window is not transparent in the wavenumber region lower than 1000 cm^{-1}. 20 μl of liposomes were mounted between CaF_2 windows with 12 μm sample thickness.

Spectra were recorded on a BOMEM 157 FTIR spectrophotometer in the temperature range of 27-70^{0}C. Before the spectrum acquisition, air inside the

spectrophotometer was purged for an hour. Between the range 27-50^{0}C, temperature was increased in steps of 2^{0}C, however, above 50^{0}C the increment was done in steps of 5^{0}C. Temperature was regulated by Unicam Specac digital temperature controller unit and a thermocouple located against the edge of the cell windows. Since the sample is heated by heating the materials surrounding it, time is needed for the sample to reach the desired temperature. For this reason, the samples were incubated for 5 minutes at each temperature before the spectrum acquisition. The samples were scanned at 2 cm^{-1} resolution for 50 times at each temperature value and they were averaged by the computer.

2.4.3. Spectral Analysis

In model membranes, the structural changes can be monitored by analysing infrared absorption bands as a function of temperature. Since, any structural change is reflected to vibrational modes of the molecule, examination of some particular absorption bands will give information about the conformation that the system is in.

One of the absorption bands that is often taken into account in most model membrane studies, is due to the carbon-hydrogen stretching vibrations in the spectral region 3100 to 2800 cm^{-1}. The strong lipid bands at 2920 and 2850 cm^{-1} are the antisymmetric and symmetric CH_2 stretching modes respectively. These bands are sensitive to differences in conformation and they reflect the changes in the trans to gauche ratio in acyl chains (Lee and Chapman, 1986). These structural changes can also be monitored by studying the bands at 2955 and 2872 cm^{-1}, which are the asymmetric and symmetric CH_3 stretching modes of the terminal methyl group

respectively. All hydrocarbon chain-melting phase transitions are accompanied by a discontinuous increase in both the maximum absorption position and bandwidths of these lipid vibrational modes. The changes reflect the increase in hydrocarbon chain conformational disorder and mobility that occur during chain-melting phase transitions (Synder, 1967).

The C=O stretching band at 1750-1700 cm^{-1} is useful for examining the interfacial region. In the structure of DPPC, this ester group is located in the polar-apolar interface and this region is sensitive to changes in the structure of the lipid molecule. Formation of new hydrogen bonds formed with the addition of drugs can be best understood by the examination of this particular band. In membranes having two acyl chains, there are two C=O bonds and hence two overlapping vibrational bands. One of the bands appears around 1742 cm^{-1} with a trans conformation and the other appears around 1728 cm^{-1}. However, in hydrated samples only a broad band contour is found and its mid-point is around 1735 cm^{-1}.

PO_2 antisymmetric stretching band arises in wavenumber region 1200-1260 cm^{-1}. This band overlaps with CH_2 wagging band. There is also a weak CH_2 rocking-twisting band at 1150-700 cm^{-1}. However, it is not possible to examine this band because CaF_2 cell used in the study is not transparent to region lower than 1200 cm^{-1}.

The O-H stretching bands due to solvent (buffer) appear in regions of 3200-3400 cm^{-1} and 1500-1800 cm^{-1}, which overlap with C-H and C=O stretching bands respectively. Therefore, it is necessary to subtract water bands from the spectrum of

61

liposomes. During the scanning of the sample, molecules in air interfere with the spectrum of the sample. Figure (2.4.3.1) shows air spectrum. In order to prevent this interfering, the spectrum of air was recorded as background and subtracted from the spectrum of sample by using the associated software of FTIR spectroscopy. Although air spectrum is automatically subtracted by the software program, subtraction of buffer spectrum is done manually. Figure (2.4.3.2) shows the infrared spectrum of DPPC liposomes before and after water subtraction.
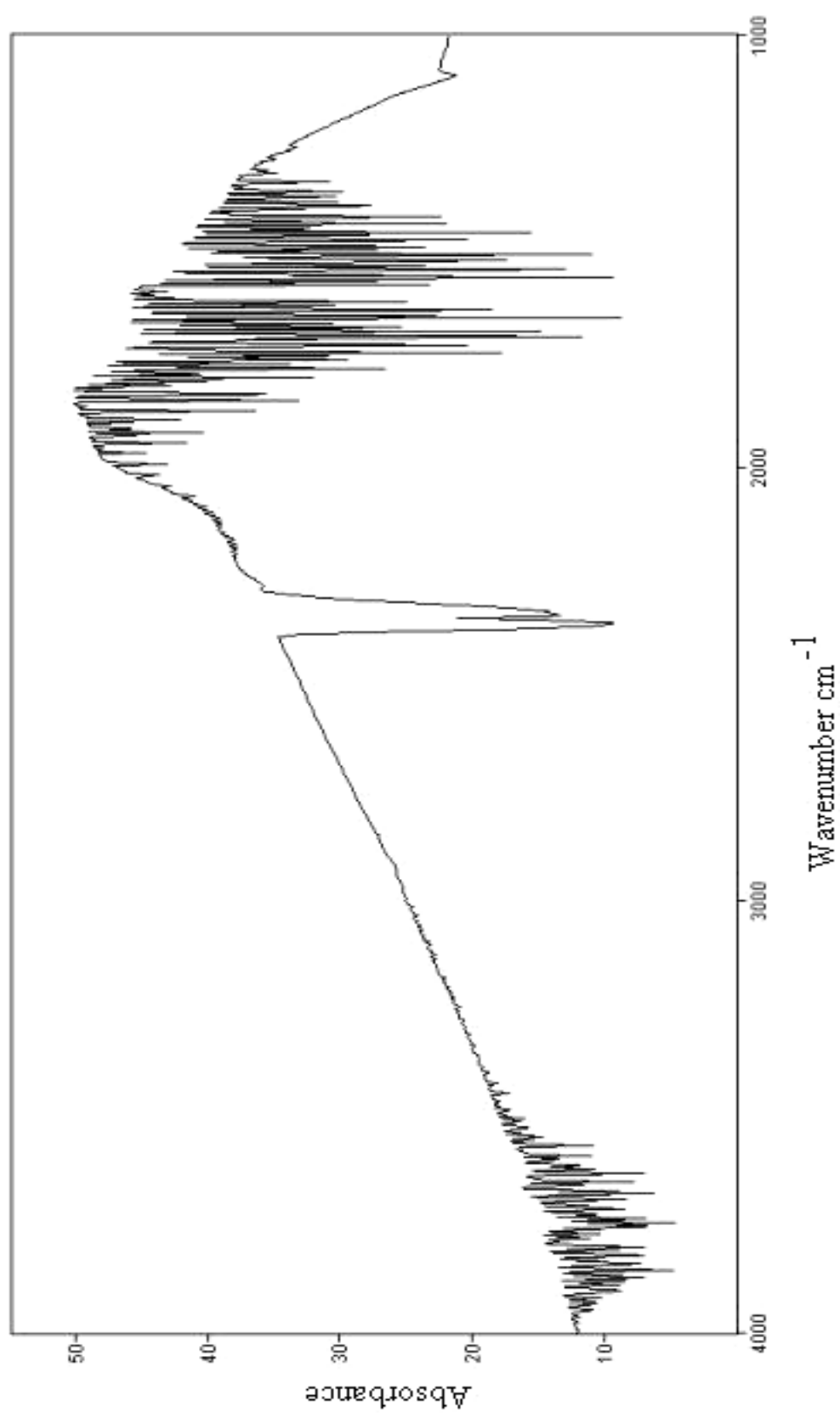
Figure 2.4.3.1 Infrared spectrum of air.
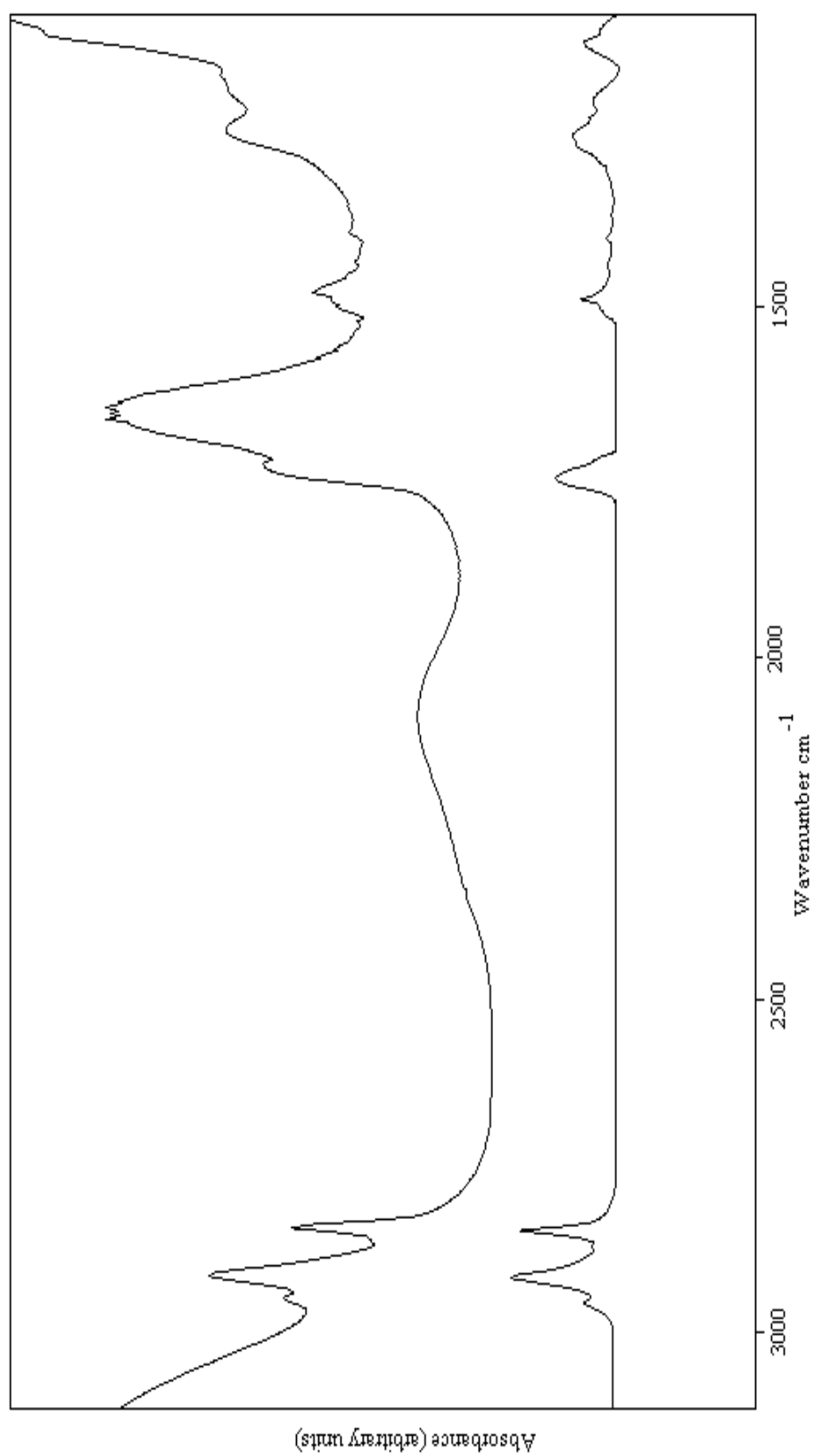
Figure 2.4.3.2 FTIR spectrum of DPPC liposomes. Upper spectrum shows the liposomes before subtraction and the spectrum below shows the liposomes after water is subtracted.

2.5. UV-Visible Spectroscopy

2.5.1. Preparation of Model Membranes

For the UV-Visible Spectroscopic analysis, thin films with or without progesterone were obtained in the same way explained for FTIR analysis but 1.5 mg lipid were hydrated by adding 1.5 ml of 10 mM phosphate buffer. Then the liposomes were formed by vortexing for 20 minutes in the same way mentioned before.

2.5.2. Sampling for UV-Visible

Plastic cuvettes, containing samples of thickness (path length) 1 cm, were used for sample holder. 1.5 ml of liposomes were placed for the analysis.

Spectra acquisitions were done by Cary 300 Bio UV-Visible spectrophotometer and a computer connected to it. Temperature was controlled by Cary Temperature Controller unit between 25-70^{0}C and it was increased in steps of 2^{0}C. The samples were incubated for 5 minutes before the spectrum was taken. Sample absorbances at wavelengths 440 nm and 550 nm were collected.

2.5.3. Spectral Analysis

Reduction in the transmitted light by scattering of molecules is called turbidity. In turbidity measurements the intensity of transmitted light is used to obtain information about the investigated system because absorbance of the system is directly proportional to the concentration of particles. In this study, two different beams of light at wavelengths 440 nm and 550 nm, which fall into visible region of electromagnetic spectrum, were used for the turbidity study. Turbidity studies give

information about fluidity of the system (Severcan et al., 1995). As the system becomes more stable, absorbance value increases. Thus, relative positions of different samples in a spectrum of absorbance versus temperature will make it possible to compare systems in terms of their fluidity.

2.6. Differential Scanning Calorimetry

2.6.1. Preparation of Model Membranes

For the calorimetric analysis, thin films containing 2 mg lipid were prepared as mentioned previously. Films were hydrated by adding 50 μl of 10mM phosphate buffer and liposome formation was done as described before.

2.6.2. Sampling for DSC

Samples were contained in aluminium pans. All the sample prepared was used for the calorimetric analysis. An empty pan was used for the reference during the analysis, so that the calorimetric effect of the pan was excluded automatically by the associated computer.

Experiments were performed with Universal TA DSC Q100 V6.21 instrument and the phase diagram was monitored by the computer. Heating rate was arranged to be 0.2 ^{0}C/min. Temperature increments were done automatically by the instrument for the interval 25-60 ^{0}C.

2.6.3 Spectral Analysis

In model membrane studies, DSC is often used for the determination of phase transition temperature and enthalpy (Bach et al., 2001; Tahir et al., 1999; Momo et al., 2002). DSC spectrum analysis gives the evidence of an interaction between the participant and model membrane, since such an interaction is reflected to the phase transition profile of the liposome. Therefore, DSC is also used for the estimation of purity and identification of materials.

Every liposome has a characteristic phase transition temperature and enthalpy value. The type of model membrane used in this study has the characteristic pretransition at 35^0C with enthalpy of 1.6 cal/g and the main phase transition at 41.2^0C with 12.5 cal/g (Mavramoustakos et al., 1997). Calibration of the instrument, the heating rate and scan rate during the experiment may cause some slight variations from the data mentioned above (Koyama et al., 2000). Phase transitions appear as a sharp peak on the DSC spectra because various structural changes of the lipid molecule in the bilayer are observed to take place within a very narrow temperature interval, so that the thermally induced phase transition occur abruptly (Figure 2.6.1). The maximum value of the peak is taken as the transition temperature of the molecule. Also, by calculating the area under the peak gives the enthalpy of the transition (Eqn. 1.4.4.1). Another parameter that is often used is the width of the peak measured from the half height in terms of temperature. This value and the transition temperature are used for obtaining information about the size and packing of cooperative units undergoing the transition. If the width is increased by the drug incorporated the bilayer, then this implies that the cooperativity of the transition is reduced (Tahir et al., 1999). Enthalpy variations show the interstitial and

substitutional impurities. Any change in transition temperature gives information about the fluidity of the system (Castelli et al., 2001). Comparison of mentioned parameters of DPPC liposomes and of liposomes containing progesterone enables us to determine the existence of an interaction.
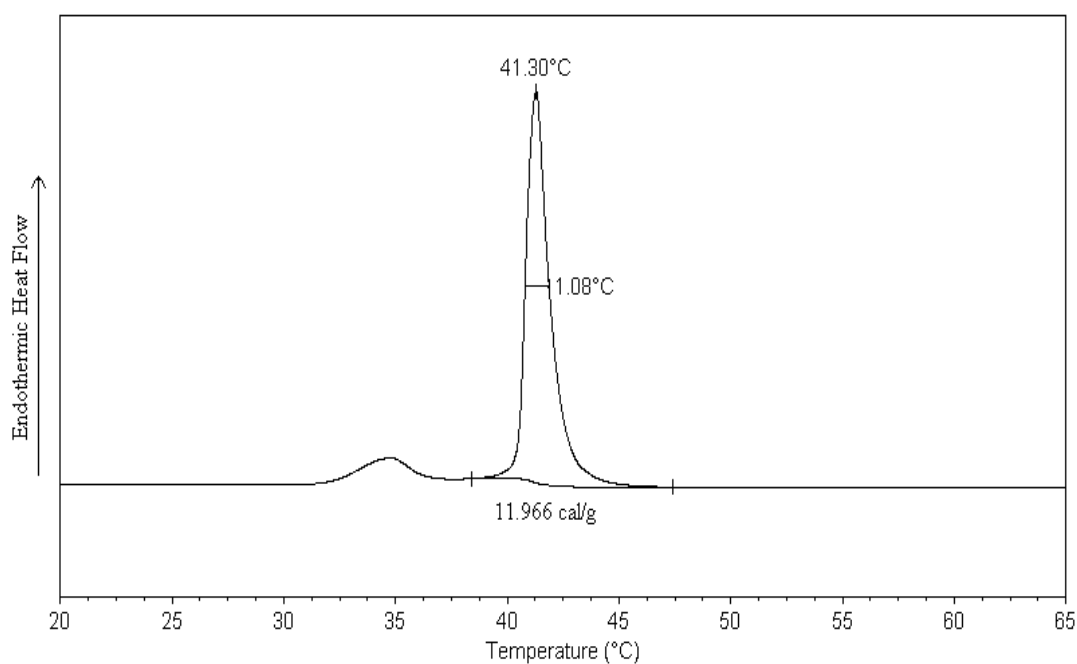
Figure 2.6.1 DSC spectra of DPPC multilamellar liposome. The first peak on the left shows the pretransition and the following peak shows the main transition. Three important parameters; namely the width at half height, temperature and enthalpy of the transition are shown on the main transition peak.

CHAPTER 3

RESULTS

The present study discusses the interaction of DPPC multibilayers with different amounts of progesterone in terms of mol%. The changes in molecular structure and dynamics were monitored by using FTIR, turbidity and DSC.

3.1. FTIR Study

In the analysis of the FTIR spectra, CH_2 symmetric and antisymmetric, C=O stretching and PO_2^- bands were studied. Figure 3.1.1 shows the infrared absorption spectra of DPPC multilamellar liposomes in the C-H stretching region at different temperatures. As it is seen from the figure, peak height, wavenumber values and the bandwidth of the bands change as the temperature of the sample is increased. These changes were measured and plotted as a function of temperature to obtain information about the system.
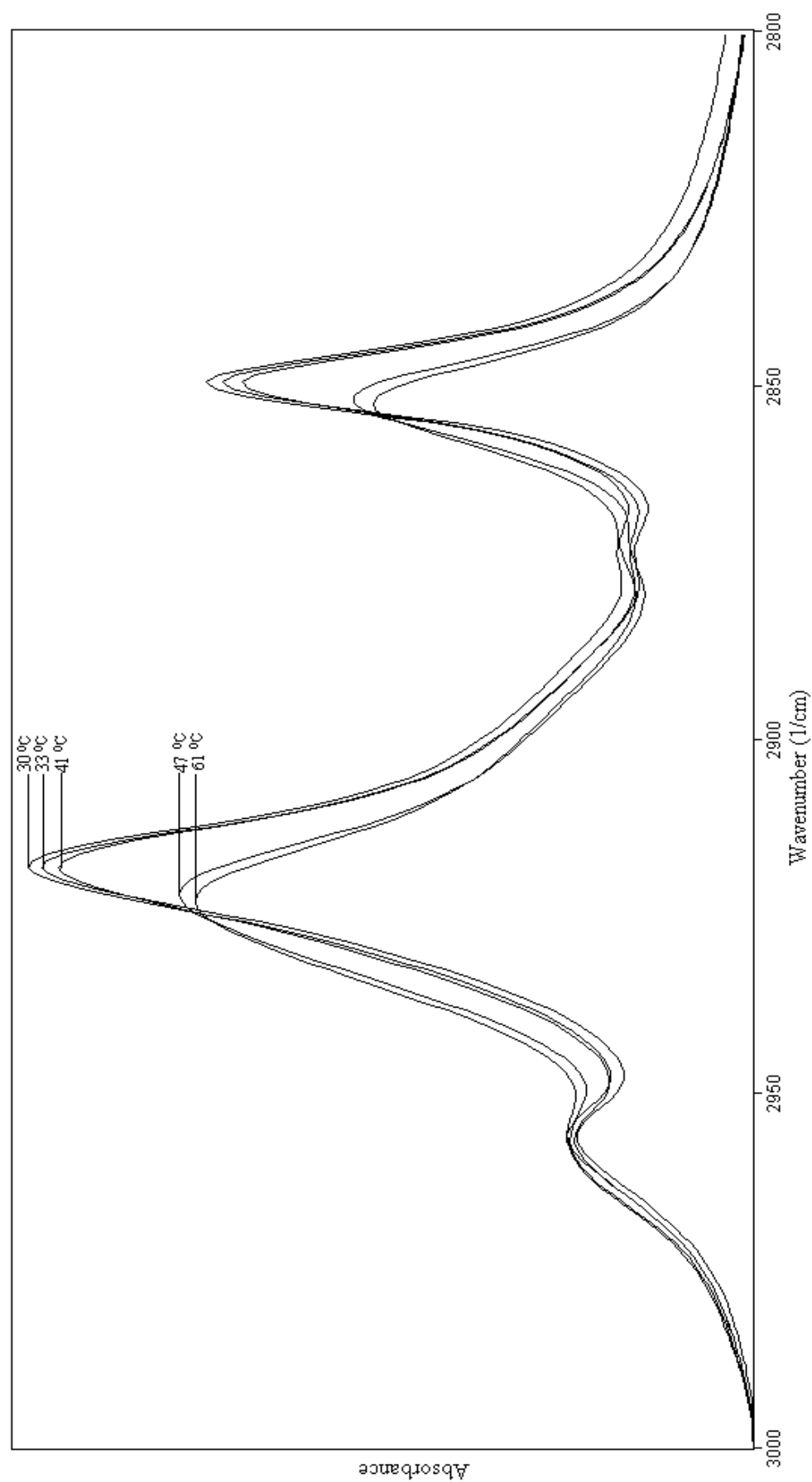
Figure 3.1.1 FTIR spectrum for the C-H stretching region of pure DPPC multilamellar liposomes.
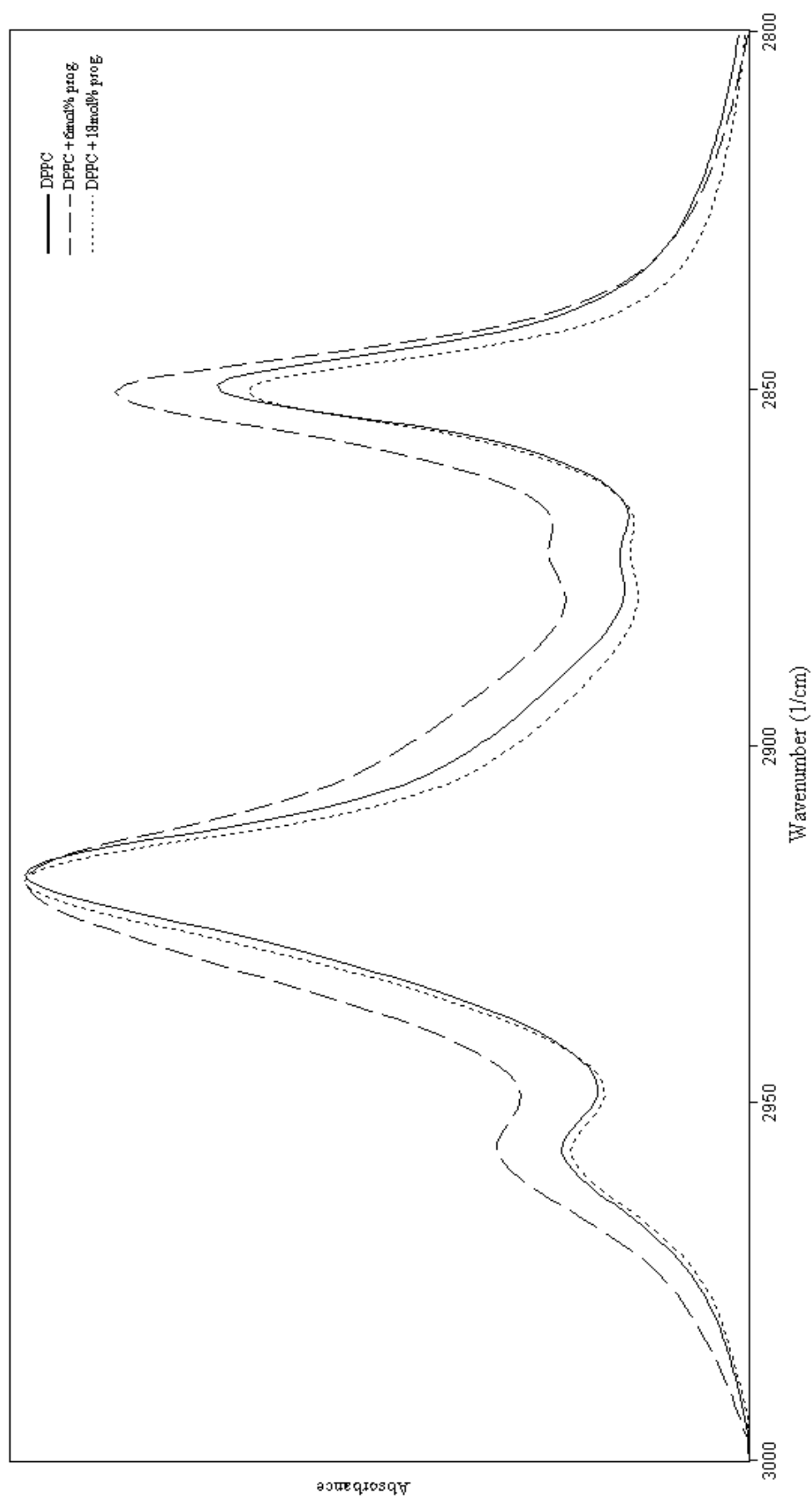
Figure 3.1.2 The Infrared spectra of DPPC liposomes in the absence and presence of progesterone in the C-H region at 41,3 ^{0}C.
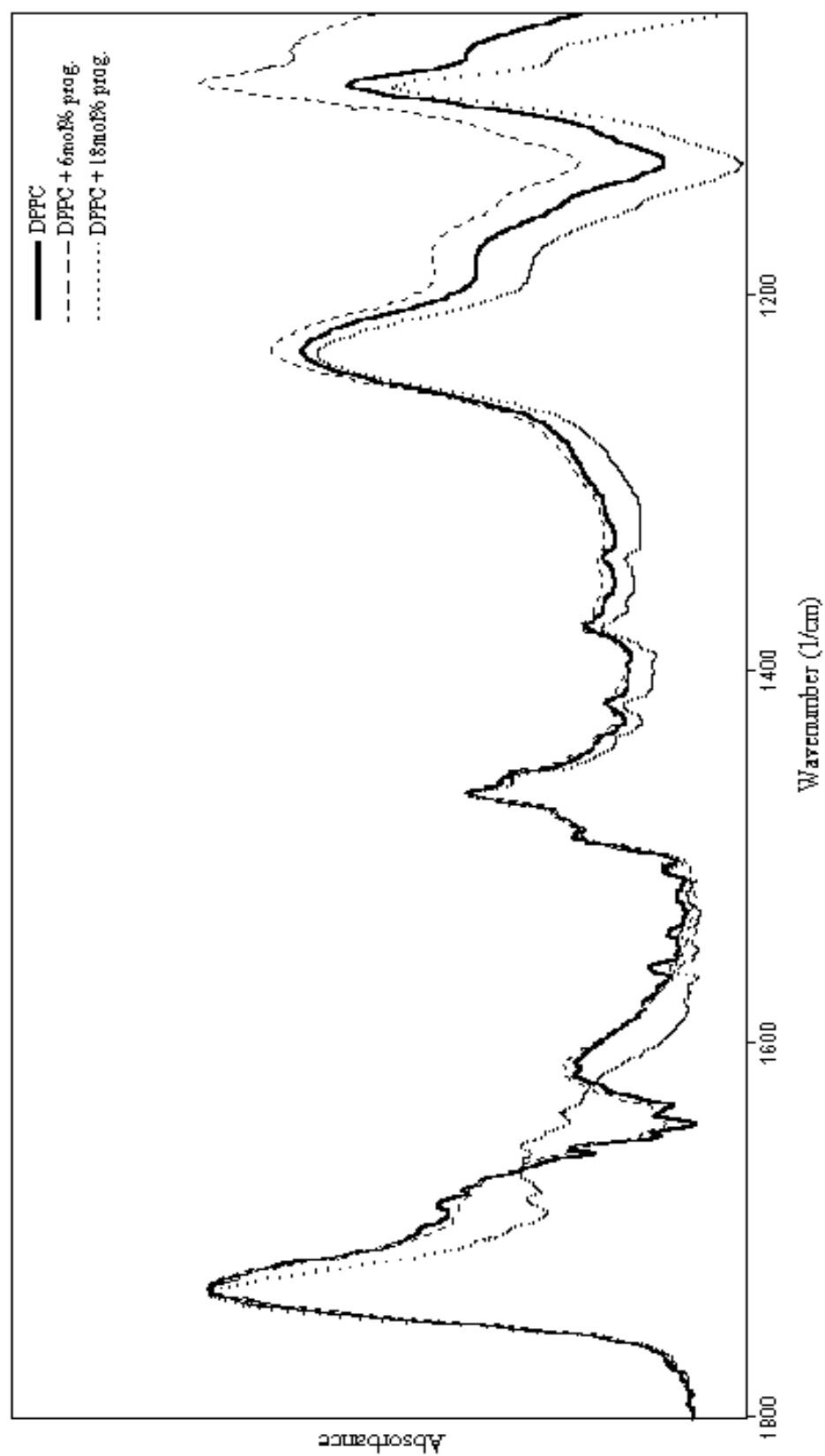
Figure 3.1.3 The Infrared spectra of DPPC liposomes in the absence and presence of progesterone in 1800-1000 cm^{-1} region at 44,3 ^{0}C.

72

In Figure 3.1.2, the effect of progesterone at low and high concentrations on lipid bands for 3000-2800 cm^{-1} region is seen. CH$_2$ symmetric stretching mode results in a peak, which is centred at 2850 cm^{-1}. The peak at 2920 cm^{-1} results from CH$_2$ antisymmetric stretching mode. CH$_3$ asymmetric stretching vibration is monitored from the peak at 2960 cm^{-1}. Figure 3.1.3 shows 1800-1000 cm^{-1} region of DPPC liposomes in the absence and presence of progesterone of low and high concentrations. The peak at 1730 cm^{-1} reflects ester bond vibrations (C=O stretching) and the peak around 1230 cm^{-1} is due to the PO$_2^-$ antisymmetric stretching vibrations. As seen from 3.1.1 and 3.1.2, progesterone alters the bandwidth, band frequencies and band intensities.

Phase transition behaviour and order-disorder state of the system are studied by the frequency analysis of C-H stretching mode as reported by Severcan et al (1996) and Toyran and Severcan (2002). Ordering of the system is reflected to spectrum as a decrease in the frequency of C-H stretching mode. Figure 3.1.4 shows temperature dependence of the CH$_2$ symmetric stretching mode of DPPC multilamellar liposomes in the absence and presence of different concentrations of progesterone.

As seen from the figure, with the addition of progesterone phase transition curve broadens. This effect is more profound for 9mol% progesterone. The main phase transition temperature (T$_t$) of pure DPPC liposome is ~41^{0}C and the pre-transition temperature is seen around 35^{0}C. T$_t$ is shifted to lower values for all the concentrations of progesterone. On the other hand, the pre-transition is completely

eliminated with the addition of progesterone. The same results were obtained for the CH$_2$ antisymmetric stretching mode (Figure 3.1.5).

Progesterone increases the frequency of oscillation, which implies a decrease in the order of the system both in the gel and liquid crystalline phase. However, the degree of disordering effect is not directly proportional to the degree of concentration of progesterone present. 1mol% progesterone slightly disorders the system. The degree of disordering effect increases clearly for all other concentrations. 9mol% of progesterone dramatically decreases the order of the system in a different manner from the others, which means the increment in the number of gauche conformers is higher than in the other concentration values. Disordering effect of progesterone is more profound in the gel phase.

Figure 3.1.4 The temperature dependence of frequency of the CH$_2$ symmetric stretching of DPPC liposomes in the absence and presence of different concentrations of progesterone.
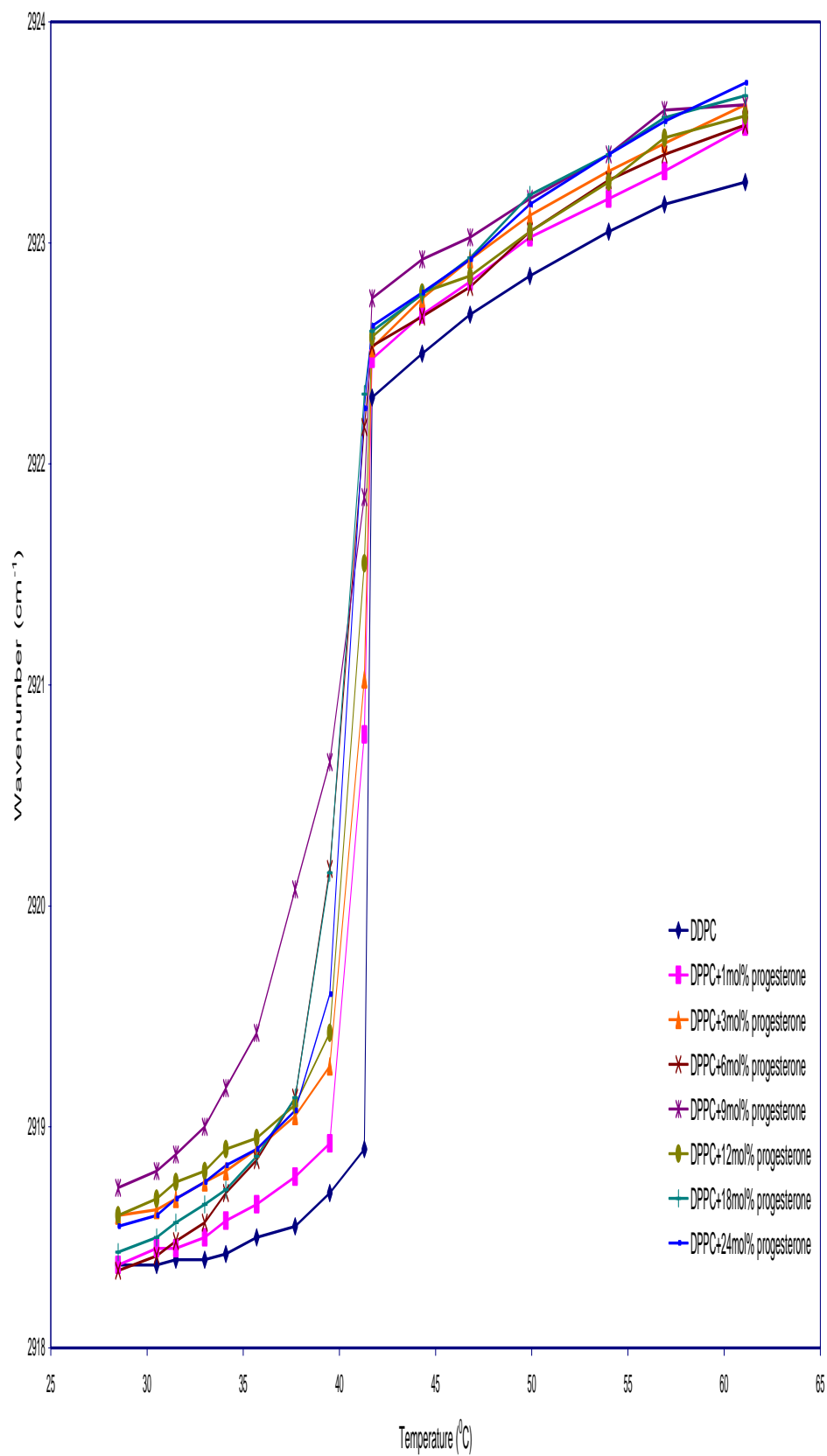
Figure 3.1.5 The temperature dependence of frequency of the CH₂ antisymmetric stretching of DPPC liposomes in the absence and presence of different concentrations of progesterone.

The temperature dependence of the CH_2 antisymmetric and symmetric stretching modes bandwidth of pure and different concentrations of progesterone containing DPPC liposomes are shown in Fig. 3.1.6 and Fig. 3.1.7 respectively. The widths were measured at 50% of height of the peaks. Bandwidth analysis gives information about the dynamics of the system. The fluidity is expected to influence bilayer permeability properties and to be required for normal and optimal activity of membrane associated proteins. The increment in bandwidth is the indication of increment of dynamics (Yi and MacDonald, 1973; Toyran and Severcan, 2002). The figures show that in gel phase 3, 6 and 9mol% progesterone values increase the dynamics of the system, whereas other concentration values have the opposite effect. It is evident from the graphs that progesterone shows dual effect on the fluidity of DPPC multilamellar liposomes according to progesterone concentrations. High concentrations of progesterone (12, 18 and 24mol%) stabilize the system, whereas low concentrations (3, 6 and 9mol%) increase the membrane dynamics. The broadening of the phase transition profile can also be seen from the bandwidth analysis.

Figure caption (below figure): DPPC liposomes in the
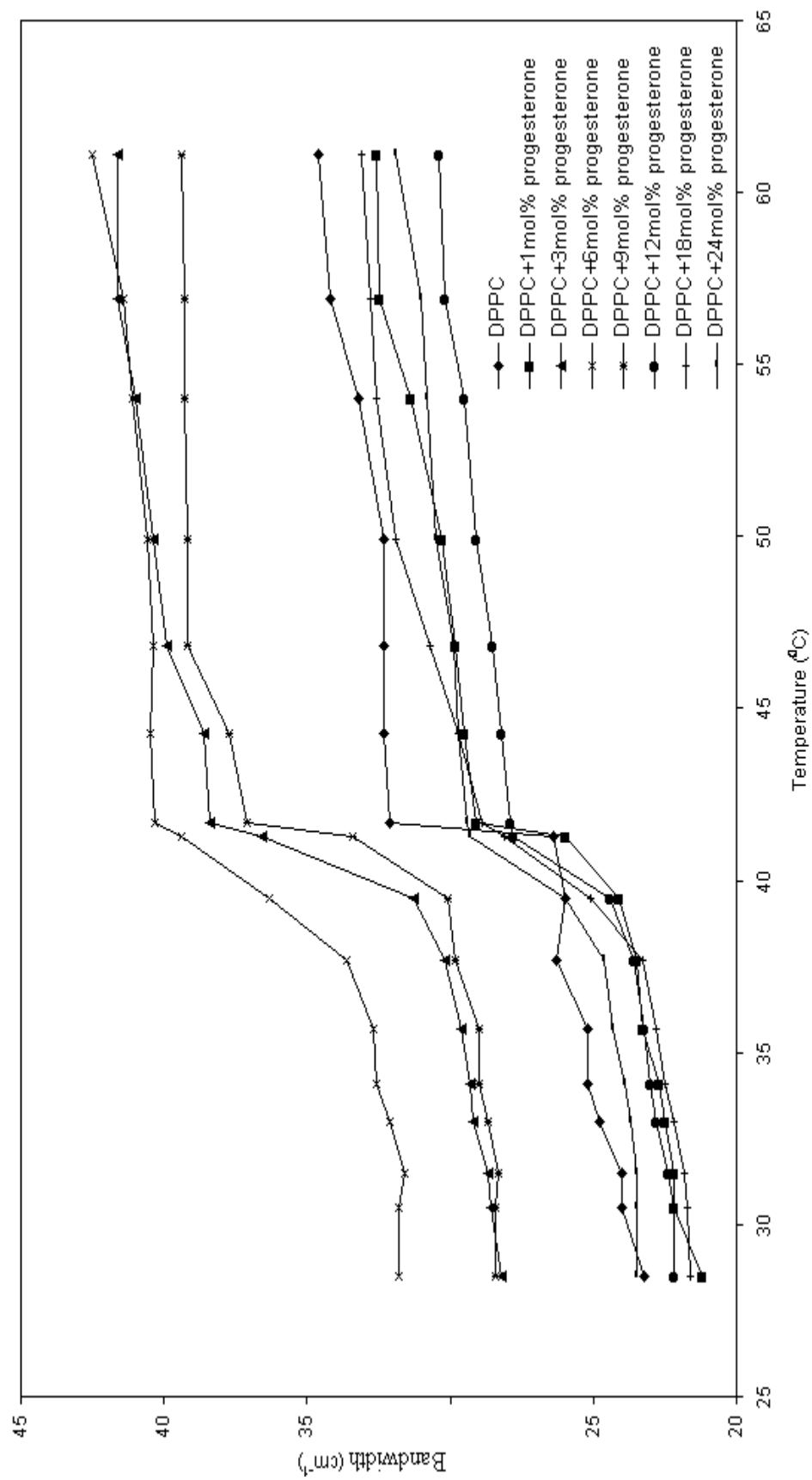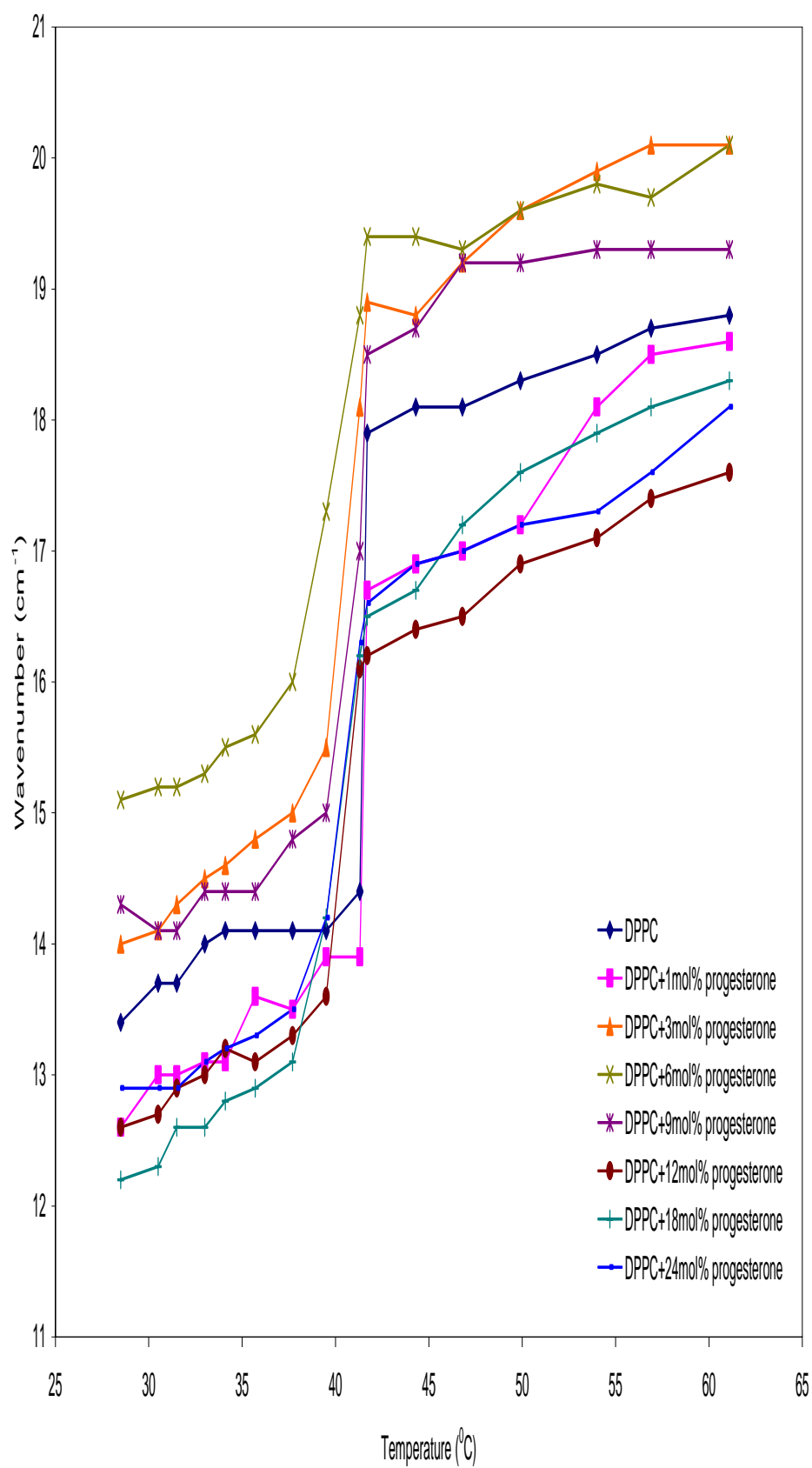
Figure 3.1.7 The temperature dependence of bandwidth of the CH$_2$ symmetric stretching of DPPC liposomes in the absence and presence of different concentrations of progesterone.

In order to examine the interaction of progesterone with glycerol backbone near the head group of phospholipids in interfacial region, C=O stretching band is analysed. The temperature dependence of the frequency of oscillation in this region is shown in Fig. 3.1.8. A decrease in frequency of oscillation implies the existence of hydrogen bonding between the components (Frengeli and Günthard, 1976). Since all the samples containing progesterone shift the frequency of oscillation to higher values, there is no evidence of hydrogen bonding, instead there are free carbonyl groups in the system. The sample containing 1mol% of progesterone has a relatively small effect in increasing the frequency but the samples in other concentrations, especially 6 and 9mol% of progesterone, highly disorders the ester group of liposomes.
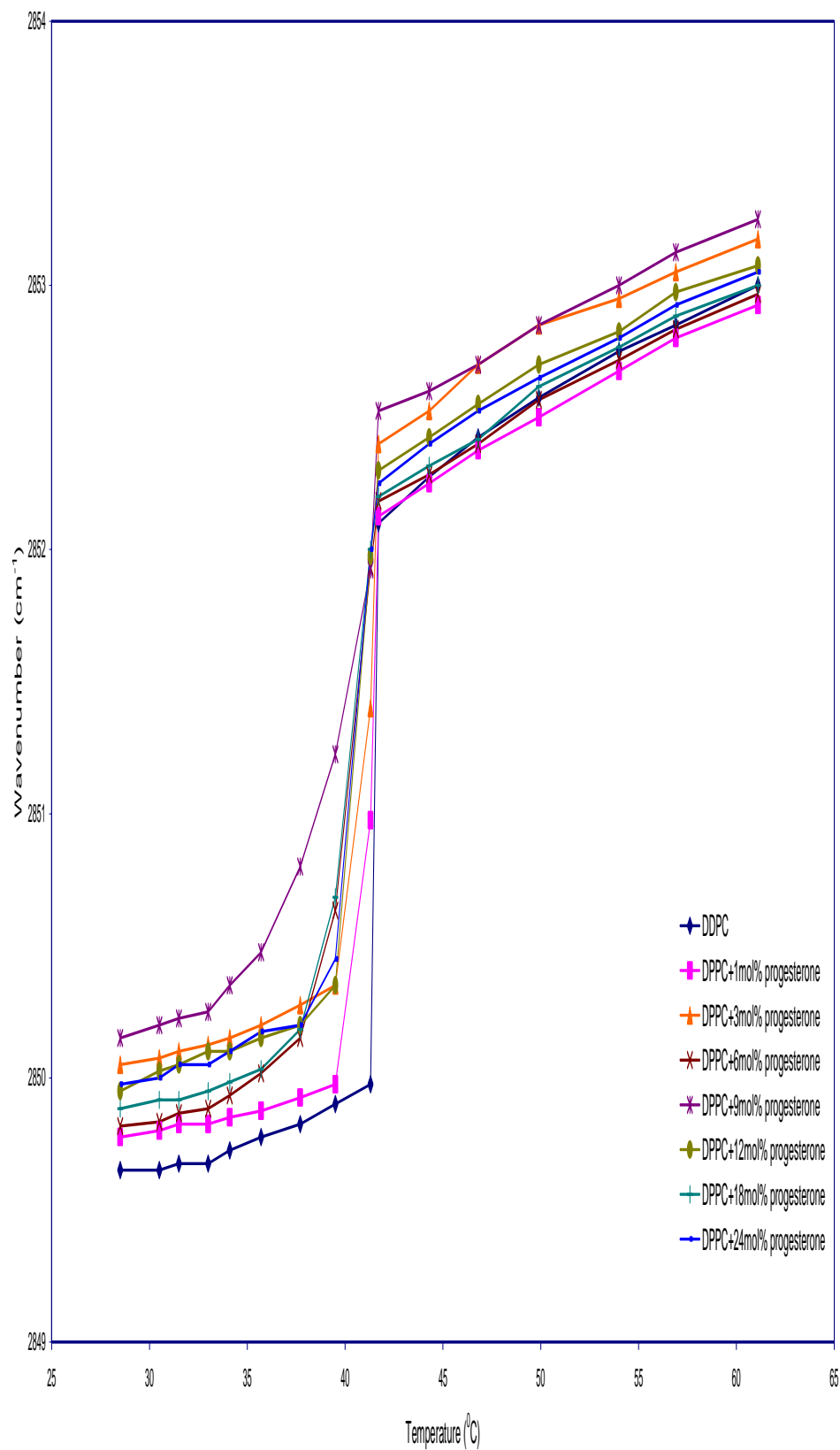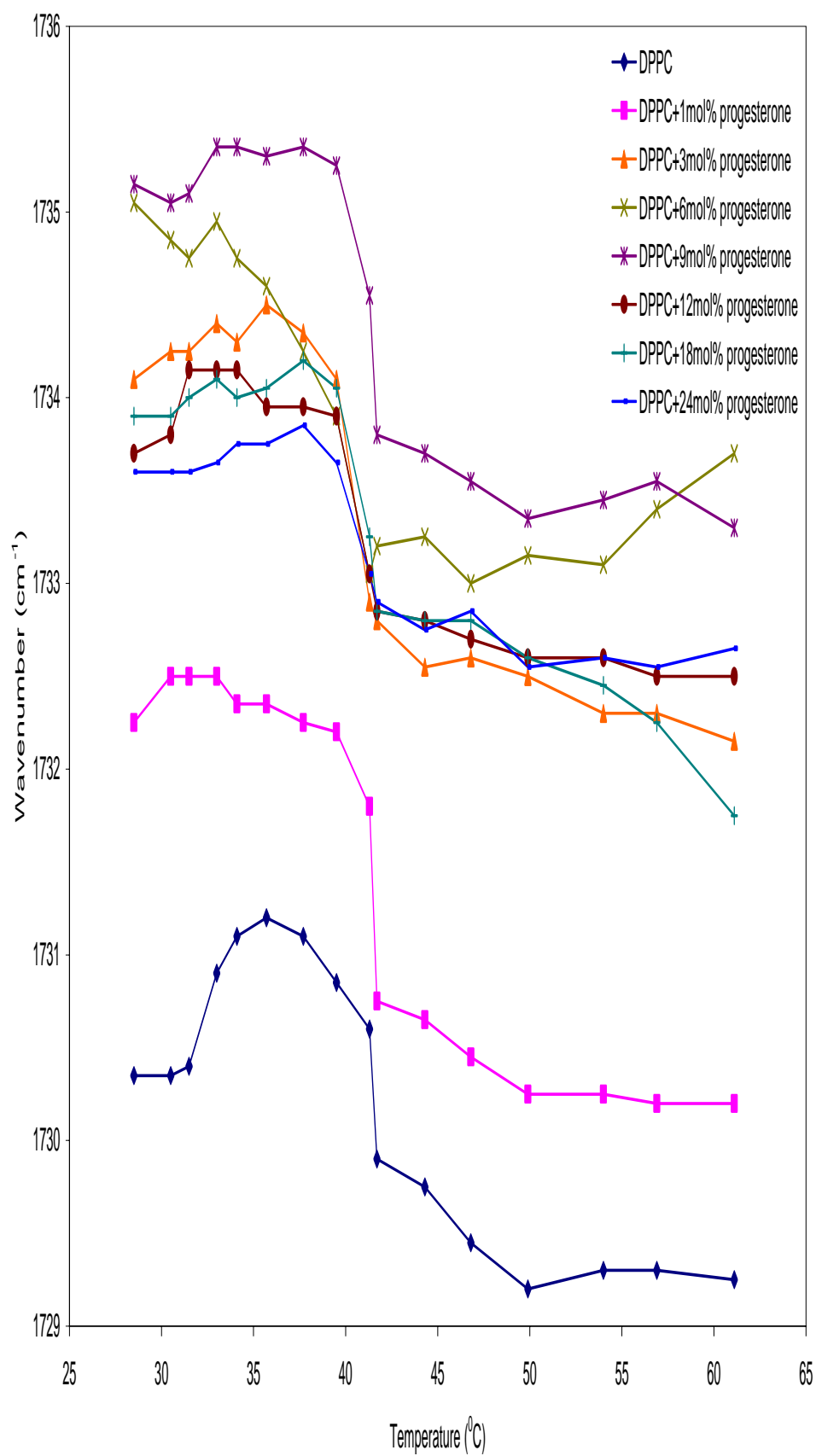
Figure 3.1.8 The temperature dependence of frequency of the C=O stretching mode of DPPC liposomes in the absence and presence of different concentrations of progesterone.

The interaction between progesterone and head group of DPPC liposomes is monitored by PO_2^- band, which is located at 1230 cm^{-1}. Figure 3.1.9 shows the PO_2^- band frequencies for DPPC liposomes in the absence and presence of different concentrations of progesterone. Vibrational energy levels shift to lower values with the formation of hydrogen bonding between the head group of liposomes and either hydroxyl group of progesterone or water molecules around.

As seen from the figure, 6mol% of progesterone shifts the wavenumber of oscillation to lower degrees in the liquid crystal phase, implying the hydrogen bond formation. However in gel phase, progesterone has no significant effect on the frequency value of phosphate head groups. It is also seen that 3mol% of progesterone decreases the frequency of oscillation in both phases. On the contrary, other concentration values increase the wavenumber of oscillation, in other words there is no hydrogen bond formation between the head group of phospholipids with the progesterone.
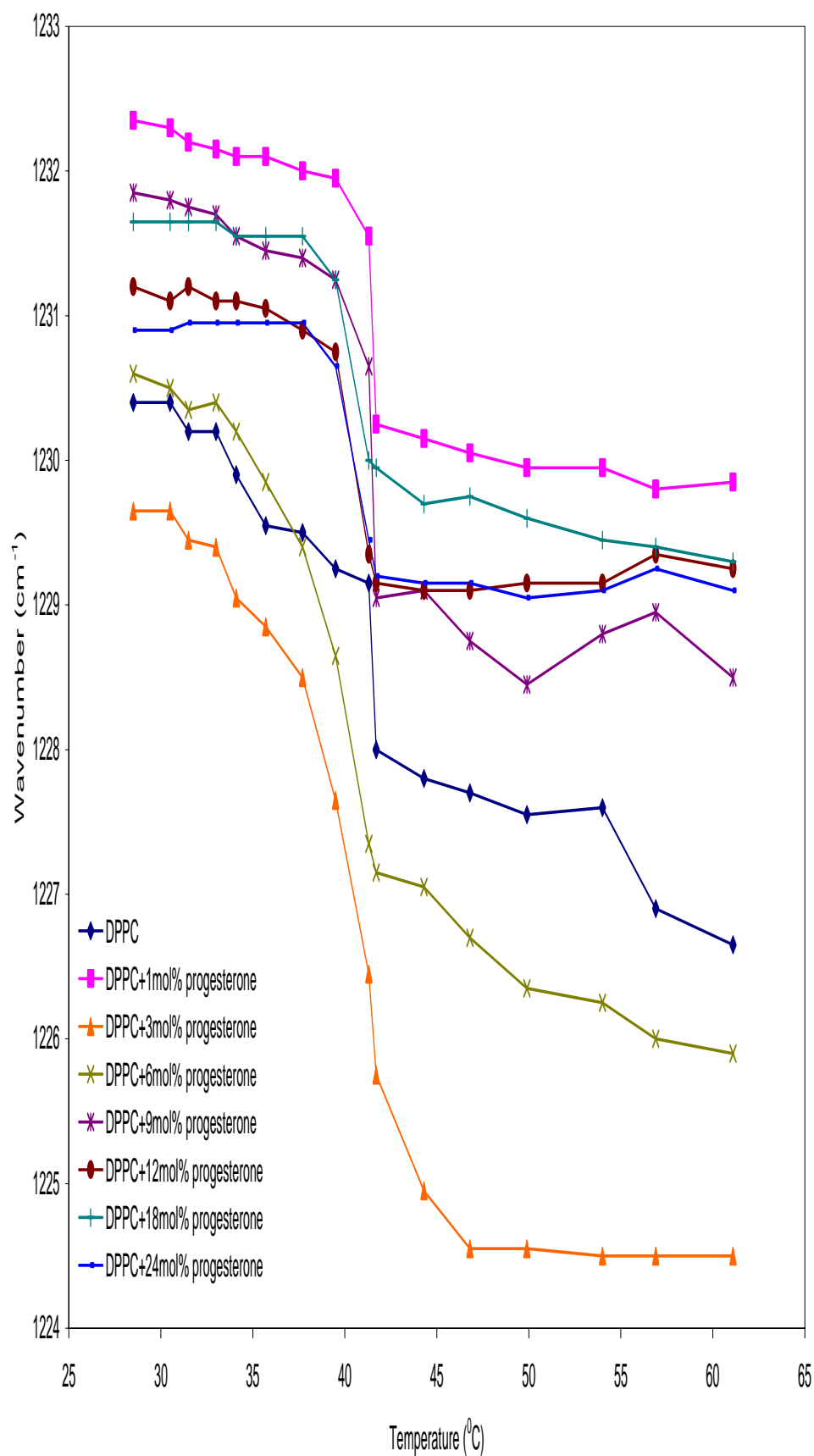
Figure 3.1.9 The temperature dependence of frequency of the PO$_2^-$ stretching mode of DPPC liposomes in the absence and presence of different concentrations of progesterone.

83

3.2 Turbidity Study

Absorbance of samples at 440nm wavelength of light, for a temperature range of 25-65^{0}C, was used for the turbidity study. Temperature dependence of absorbance of DPPC multilamellar liposomes in the absence and presence of progesterone in different mol% concentrations are shown in Figure 3.2.1. Turbidity study is used in order to obtain information about the fluidity of the system (Severcan et al., 1995; Kazancı et al., 2000). The increase in absorbance value implies a decrease in lipid dynamics. In the light of this information, it is seen from the figure that low concentrations of progesterone (1-9mol%) increase the fluidity of the liposomes in both gel and liquid crystalline phase. However, other concentration values make the liposomes more stable in both phases.

It is also seen that phase transition curve is slightly broadened upon the addition of 9mol% of progesterone. Furthermore, the phase transition temperature is decreased with the addition of progesterone; most considerably by 6 and 9mol% of progesterone concentrations.
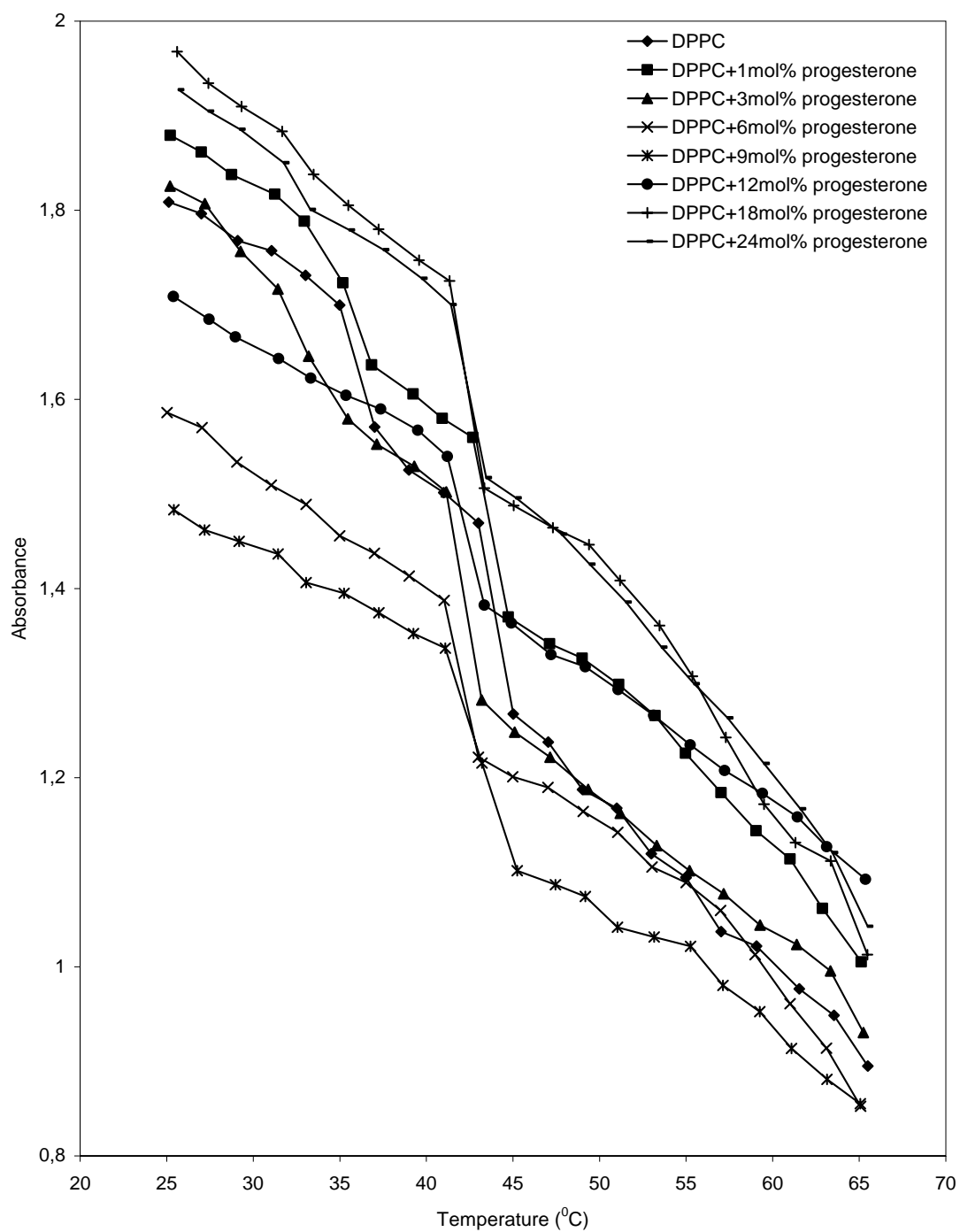
Figure 3.2.1. Temperature dependence of absorbance at 440 nm for DPPC liposomes in the absence and presence of progesterone.

3.3. DSC Study

Calorimetric investigation of DPPC multilamellar liposomes with or without progesterone was carried out for a temperature range of 25-60^{0}C. The corresponding heating flow as a function of temperature curve is shown in Figure 3.3.1. The thermotropic properties of hydrated DPPC liposomes have extensively been studied by DSC method (Melchior and Stein, 1976; Huang and Li, 1999). The characteristic parameters used for obtaining information in lipid studies are the enthalpy, width at half height and the phase transition temperature. As shown in Figure 3.3.1, DPPC liposomes show the characteristic pretransition with a low-enthalpy change and a sharp main transition at 35.2^{0}C and 41.2^{0}C respectively (Mavramoustakos et al., 1997). In our study the pretransition and main transition temperature were determined as 33.7^{0}C and 40.9^{0}C, respectively.
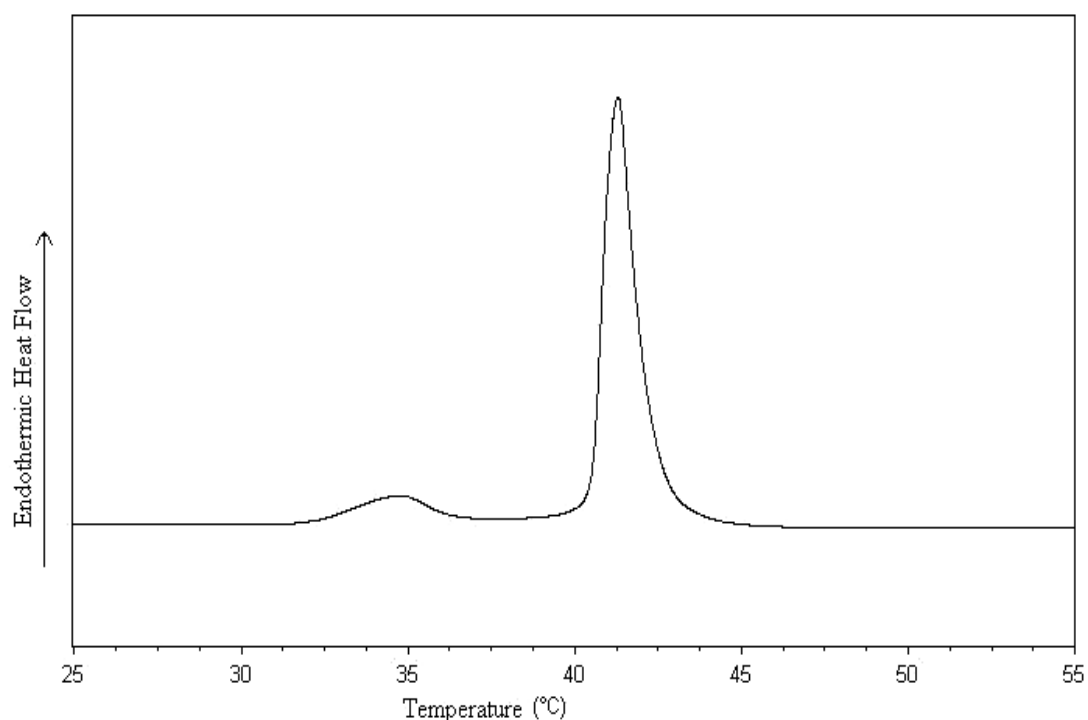
Figure 3.3.1 DSC spectrum of DPPC liposomes. The small peak at around 34^0C shows the pretransition and the big peak at 41^0C shows the main transition.

According to Figure 3.3.2, transition temperatures decrease as progesterone concentration is increased. All the concentration values of progesterone made the transition peaks broader, which means addition of progesterone disorders DPPC liposomes. This result is in agreement with infrared spectroscopy of CH_2 stretching frequency analysis, which also gives order information about the system.

For concentrations of 6 and 12mol% progesterone, a shoulder is seen on the transition peaks and in 9mol% of progesterone two peaks resulted in a very broad single peak, implying a lateral phase separation of liposomes for these samples. Also all the samples including progesterone eliminated the pretransition of liposomes.

Table 3.3.1. Width at half height (ΔT), transition temperatures (T_t) and enthalpy of the transitions (ΔH) are given.

Samples	ΔT (^{0}C) (at half height)	T_t (^{0}C)	ΔH (cal/g)
DPPC	0,18	40,9	11,04
DPPC+1mol% prog.	0,24	40,7	12,80
DPPC+3mol% prog.	0,47	40,4	11,00
DPPC+6mol% prog.	0,94	39,7	7,84
DPPC+9mol% prog.	1,28	38,4	7,53
DPPC+12mol% prog.	1,61	39,6	9,84
DPPC+18mol% prog.	0,99	39,9	11,01
DPPC+24mol% prog.	1,17	39,5	9,48

The width of the peaks in terms of temperature, the transition temperatures and enthalpies of all the samples are given in Table 3.3.1. When the enthalpies of samples are compared, it is found that the enthalpy of transition is severely decreased in the cases of 6 and 9mol% of progesterone. At these concentrations the system is destabilized or in other words, more fluid. This result is also in agreement with the results obtained by turbidity study and CH_2 stretching bandwidth analysis of FTIR.
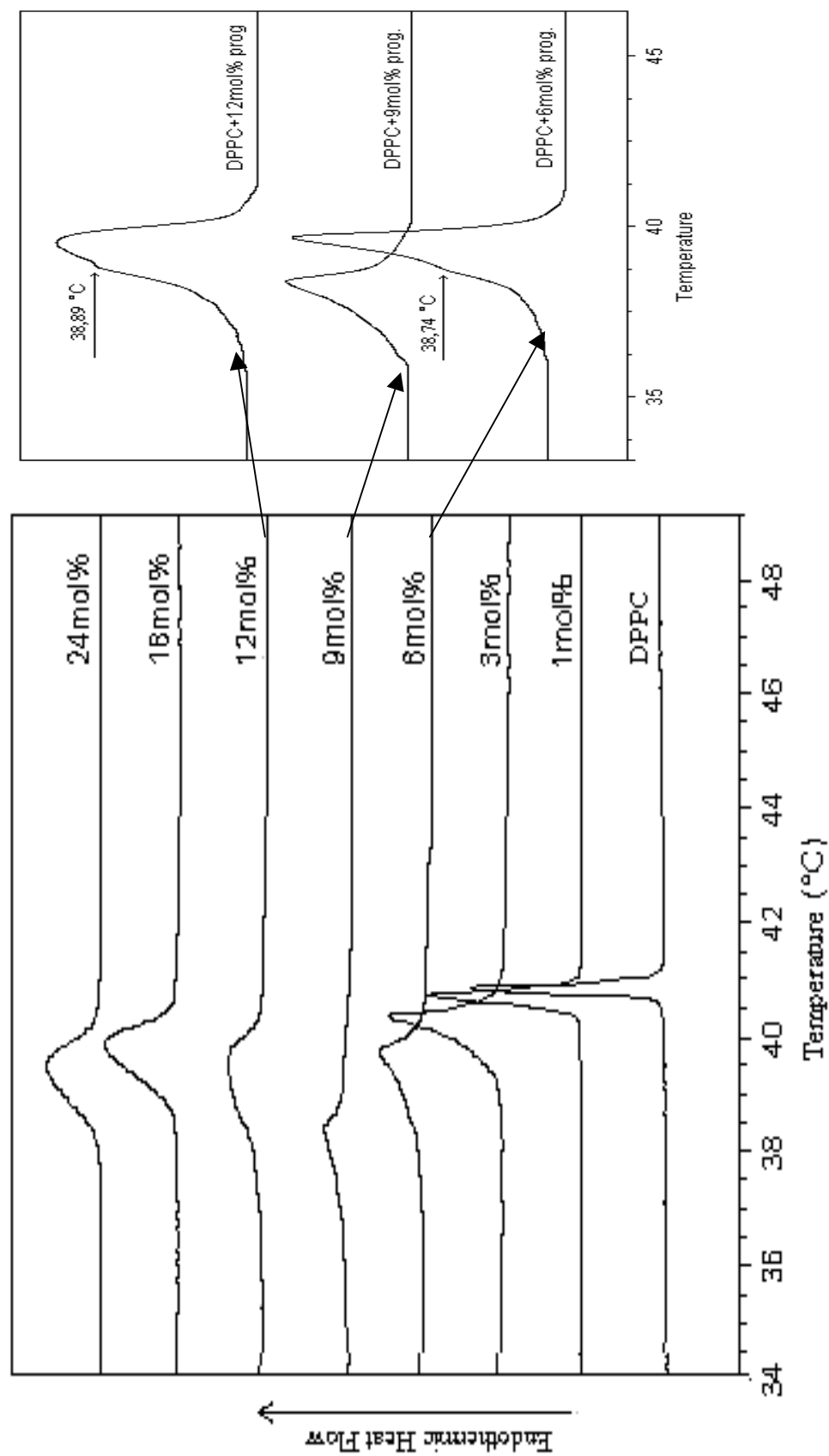
Figure 3.3.2 DSC spectra of DPPC liposomes in the absence and presence of progesterone with different mol% concentrations.

CHAPTER 4

DISCUSSION

The effect of progesterone on the phase transition profile, order and dynamics of DPPC multilamellar liposomes was monitored by non-perturbing techniques such as infrared spectroscopy, turbidity at 440 nm and DSC. In this chapter, experimental results will be discussed. Every experiment was repeated three times and similar trends were observed in each case.

We were particularly carefull in distinguishing between structural parameters describing molecular order and motion parameters such as bandwidth describing molecular dynamics as suggested by others (Ginket et al., 1989).

4.1 Progesterone-DPPC Model Membrane Interaction

In the present study, it is the first that we investigated in detail the effect of progesterone on lipid phase transition, order and dynamics and hydration states of the head and the region near the head groups of zwitterionic DPPC MLVs as a function of temperature and progesterone concentration varying from low (1mol%) to high (24mol%). Furthermore, it is the first that the existence of lateral phase separation in

binary mixture of progesterone and DPPC at lower concentration of progesterone has been shown in this study. In addition, we showed for the first time the opposite effect of progesterone on membrane dynamics at low and high progesterone concentrations.

The infrared spectra of DPPC MLVs, both pure and containing different concentration of progesterone varying from 1mol% to 24mol%, were investigated as a function of temperature. The C-H stretching modes at 2800-3000 cm^{-1}, C=O stretching mode at 1735 cm^{-1} and PO_2^- antisymmetric stretching double bands at 1220-1240 cm^{-1} were considered.

Progesterone induces shifts in the peak position of the FTIR bands and changes in the bandwidths of several bands in comparison to those of DPPC liposomes. These changes can be used to extract information about various physicochemical procesess taking place in the system. For example, the frequencies of the CH$_2$ stretching bands of acyl chains depend on the degree of conformational disorder and hence the frequencies can be used to monitor the average trans/gauche isomerization in the systems. The shifts to higher wavenumbers correspond to an increase in number of gauche conformers (Toyran and Severcan, 2003; Casal and Mantsch, 1984; Severcan, 1997; Villalain, 1986). Furthermore the bandwidths of the CH$_2$ stretching bands give dynamic information about the system (Toyran and Severcan, 2003; Villalain, 1986; Casal, 1980; Lopez-Garcia et al., 1993; Kazancı, 2001).

By monitoring the CH_2 stretching vibrations in FTIR spectra, we showed that progesterone increrases acyl chain flexibility i.e. increases disorder of DPPC membrane both in the gel phase and in the liquid crystalline phase (Fig.3.1.4.). Our results are in agreement with a recent spin label ESR study on progesterone-erthrocytes membrane interactions in where a decrease in membrane order was reported at 37 °C (Tsuda et al., 2002).

A dramatic increase in the dynamics of DPPC membranes is observed in the presence of lower concentration of progesterone (3, 6 and 9mol%) both in the gel and liquid crystalline phase (Fig.3.1.6 and 7). However for other concentrations a decrease in dynamics is observed. These results are further supported by turbidity studies where we also observed a dramatic increase in lipid fluidity especially for 6 and 9mol% progesterone.

The changes in the frequency and in the bandwidth with respect to temperature are not concerted for high concentrations of progesterone since it induces a decrease in the order and at the same time a decrease in the dynamics of the membrane. This type of behaviour has been previously reported for cholesterol containing phospholipid membranes (Van Ginkel et al., 1989).

There is a limited number of study in the literature about the effect of progesterone on membrane dynamics (Whiting et al., 2000; Liang et al., 2001; Tsuda et al., 2002). The results of these studies are not in agreement with each other. Whiting et al. (2000), using steady state fluorescence polarization, reported that

92

progesterone decreases lipid fluidity in both egg yolk phosphatidylcholine and natural membranes. In their study, they used high concentrations of progesterone (>10mol%). Their findings are in agreement with our results since we observed a decrease in membrane dynamics at high concentrations of progesterone. Liang et al. (2001) also observed a decrease in membrane dynamics in liposomes and cells using fluorescence spectroscopy. In contrast to this, recently Tsuda et al. (2002) reported an increase in membrane dynamics in a progesterone concentration dependent manner, in erythrocytes membranes at very low progesterone concentrations.

FTIR and DSC results reveal that progesterone eliminates pretransition and shifts to main transition to lower temperatures which is in agreement with a previous study (Carlson et al., 1983). We observe that with the addition of progesterone, the main DSC curve (around 41^0C) decreases in intensity and broadens. This may suggest the co-existence of more than one domain. If these domains are sufficiently large, the exchange of lipids between the domains can not be resolved and DSC curve will be a superimposition of more than one component. As progesterone concentration is increased to 6mol%, more than one peak appears in the calorimetric profile, indicating that phase separation of lipids are indeed occurring probably producing phases with different ratios of progesterone and phospholipids. In the presence of 12mol% progesterone, the main peak is clearly resolved into two components. It is also observed that intensity of the peak located at lower temperature increases in the presence of 12mol% progesterone. This peak seems to arise from progesterone rich domains and the other peak located at higher temperatures may arise from progesterone poor domains. Previous studies also

reported the existence of two different phases on the binary mixture of phospholipids and drugs such as Vitamin E (Severcan and Cannistraro, 1988) and Vitamin D_2 (Kazancı et al., 2001), Vitamin D_3 (Bondar, 1995).

FTIR also enables us to monitor hydrophilic part of the bilayer i.e. the head and the region to polar head group of phospholipid (Severcan et al., 2000). Progesterone is also found to make no hydrogen bonds in the interfacial region of the bilayer, which is monitored by C=O stretching vibrations. It is possible that progesterone displaces some H_2O molecules from the interfacial region resulting in an increase in the number of free carbonyl groups. The lack of C-H chain and hydroxyl group in A-ring in the structure of progesterone can be the reason for not making hydrogen bond with DPPC liposomes (Dimitrov and Lalchev, 1998).

In the analysis of head group (PO_2^-) vibrations, distinct effects between different concentration values were observed. While 3mol% of progesterone decreases the head group vibration frequency of the membrane, 6mol% of progesterone lowers the frequency only in the liquid crystal phase of the bilayer. In contrast to this, other concentrations of progesterone increase the frequency of oscillation. PO_2^- molecules are highly sensitive to changes in hydration (Casal et al., 1987). Since, progesterone has no hydroxyl group in A-ring; PO_2^- molecules are probably forming hydrogen bonds with water molecules around in the vicinity of progesterone.

A change in transition temperature of liposomes is related with the cooperativity of the lipid molecules of liposome (Güldütuna et al., 1997). Loss in cooperativity of lipids means the break down of van der Waals forces between the lipid molecules. This leads to the formation of progesterone-rich and progesterone-poor domains as suggested before. These two domains make the main phase transition occur at slightly different temperatures, causing a lateral phase separation. Phase separation can be understood by a shoulder appearing on the main transition peak or by an extra peak around it (Shaikh, et al. 2001; Bach et al. 2001). Molecules can interact with lipids in liposomes by inserting themselves into the bilayer of membrane, taking the place of lipid molecules and such an interaction cause simultaneous T_t variation and ΔH change (Lee, 1977; Cater et al., 1974). The broadening of peak profile and lowering of transition temperature demonstrate that both the size and packing of bilayers are modified, and the system is disordered (Jain and Min Wu, 1977; Momo et al. 2002). The lack of cooperativity together with the broadening of transition peak imply the penetration of drug into the hydrophobic core of the bilayer (Van Osdol et al., 1992), which was also revealed by infrared spectroscopy of CH_2 frequency analysis. Our results support the previous study reported by Bueno et al. (1990). Conflicting this and our study, Carlson et al. (1983) reported that progesterone is mainly associated with the hydrophilic region of membrane. The location of progesterone in adjacent to a double bound or ester moiety in lipid molecules was also proposed by NMR studies (Sanchez-Bueno et al., 1990).

CONCLUSION

The present work firstly investigated the effect of the steroid hormone, progesterone, on the physical properties, such as phase transition, membrane order and dynamics, of pure neutral (DPPC) model membrane as a function of progesterone concentration and temperature.

In this study three non-invasive techniques, namely FTIR spectroscopy, turbidity technique at 440 nm and DSC were used. By using FTIR we were able to monitor different parts of the membrane such as the head group, acyl chain and the interfacial region. We were able to obtain information about these regions of the membrane in terms of interactions.

There are contradicting results in literature about the membrane fluidity and the location of progesterone in membrane. Results obtained in this study reveal that there is strong interaction between progesterone and lipid membranes. In the present study, it has for the first time been shown that progesterone makes opposite effects on membrane fluidity at low (3, 6 and 9mol%) and high concentrations (12, 18 and 24mol%). It disorders the system in both phases for all concentrations. Furthermore, we showed for the first time that it induces phase separation at lower concentrations (3-12mol%). Evidently, these interactions are dependent on concentration of

progesterone and temperature. Generally, it has been observed that progesterone disorders the acyl chain of DPPC liposomes. In addition, cooperativity of lipid molecules are modified by affecting the van der Waals forces among the lipid molecules, thus pretransition is completely diminished, the phase transition profile and temperature is considerably changed. Progesterone showed its effect on acyl chains rather than the head group or interfacial region of DPPC liposomes. Due to the lack of hydroxyl group and C-H chain in progesterone structure, it does not bind to the hyrdophilic part of the membrane and therefore reaches the deep interior of the bilayer. This leads to the conclusion that progesterone intercalates to the hydrophobic core of the membrane

REFERENCES

A Comprehensive Introduction to Membrane Biochemistry, Datta,D.B. Floral Publishing, Madison, 1987.

Andreoli,T.E., Hoffman,J.F., Fanestil,D.D. and Schultz,S.G. (1986) In: Physiology of Membrane Disorders. Plenum Medical Book Company, New York and London.

Anton P. J. Middelberg, A.P.J., Radke, C.J., and Blanch, H.W. (2000) Peptide interfacial adsorption is kinetically limited by the thermodynamic stability of self association. Proc. Natl. Acad. Sci. USA., 97 (10), 5054–5059.

Babetta, L. Marrone, Gentry, R.T., and Wade, G.N. (1976) Gonadol hormones and body temperature in rats: Effects of estrous cycles, castration and steroid replacement. Physiology&Behavior 17, 419-425.

Bach, D., Borochov, N., and Wachtel, E. (2001) Phase separation of cholesterol and the interaction of ethanol with phosphatidylserine-cholesterol bilayer membranes. Chemistry and Physics of Lipids 114, 123-130.

Badenoch-Jones,P. and Baum,H. (1973) Progesterone-induced permeability changes in rat liver lysosomes. Nature 242, 123.

Baulieu, E.E., Godeau, F., Schorderet, M. and Schorderet-Slatkine, S. (1978) Steroid-induced meiotic division in xenopus laevis oocytes: surface and calcium. Nature 275, 593-598.

Beato,M. (1989) Gene regulation by steroid hormones. Cell 56, 335– 344.

Biochemistry, Edited by Geoffrey Zubay. Addison-Wesley Publishing Company Incorporation, 1983.

Biological Spectroscopy, Edited by B. Liguori. Benjamin/Cummings Publishing Company, Inc., 1984.

Biology, Johnson,R., Fifth edition. The McGraw-Hill Companies, Inc. 1999.

Biomembranes: Molecular Structure and Function, Gennis,R.B. Springer Advanced Texts in Chemistry, 1989.

Bitran, D., Shielch, M., McLead, M. (1995) Anxiolytic effect of progesterone is mediated by the neurosteroid alloprognanolone at brain $GABA_A$ receptors. J. Neuroendocrinol. 7, 171-177.

Bondar, O.P., Rose, E.S. (1995) Differential scanning calorimetry study of the effect of Vitamin D_3 on the thermotropic phase behaviour of lipids model systems. Biochim. Biohys. Acta 1240, 125-132.

Borgese, F., Sardet, C., Cappadoro, M., Pouyssegur, J., and Motais, R. (1992) Cloning and Expression of a cAMP-Activated Na+/H+ Exchanger: Evidence that the Cytoplasmic Domain Mediates Hormonal Regulation. Proc. Natl. Acad. Sci. USA. 89 (15), 6765–6769.

Brann,D.W., Hendry,L.B., and Mahesh,V.B. (1995) Emerging diversities in the mechanism of action of steroid hormones. J.Steroid Biochem.Molec.Biol. 52, 113-133.

Brown, W.H., Christopher, S.F., Organic Chemistry, Second Edition. Saunders College Publishing 1998.

Burke, C.R., Macmillan K.L., and Boland M.P. (1996) Oestradiol potentiates a prolonged progesterone-induced suppression of LH release in ovariectomised cows. Animal Reproduction Science, Volume 45, 13-28.

Cagnacci, A., Volpe, A., Paoletti, A.M., and Melis, G.B. (1997) Regulation of the 24-hour rhythm of body temperature in menstrual cycles with spontaneous and gonadotropin-induced ovulation. Fertility and Sterility 68, 421-425.

Campbell,I.D. (1984) In: Biological Spectroscopy Edited by Elias,P. The Benjamin/Cummings Publishing Company, Inc.

Carlson, J.C., Gruber, M.Y. and Thompson, J.E. (1983) A study of the interaction between progesterone and membrane lipids. Endocrinology 113, 190-194.

H.L. Casal, Biochemistry 19 (1980) 444.

Casal,H.L. and Mantsch,H.H. (1984) Polymorphic phase behaviour of phospholipid membranes studied by infrared spectroscopy. Biochim.Biophys.Acta 779, 381-401.

Casal,H.L., Mantsch,H.H, Paltauf, F. and Hauser, H. (1987) Infrared and 31P-NMR studies of the effect of Li+ and Ca2+ on phosphatidylserines. Biochim. Biophys. Acta 919, 275-286.

Castelli, F., Librando, V., and Sarpietro, M.G. (2001) A calorimetric evidence of the interaction and transport of environmentally carciogenic compounds through the biomembranes. Thermochimica Acta 373, 133-140.

Cater, B.R., Chapman, D., Hawes, S.M. and Saville, J. (1974) Lipid phase transitions and drug interactions. Biochim Biophys Act 363(1), 54-69.

Chemical Analysis; Modern Instrumentation Methods and Techniques, Edited by F. Rouessac and A. Rouessac. John Wiley and Sons, Ltd., 2000.

Continuous and Discrete Signals and Systems, Edited by T. Kailath. Prentice-Hall Incorporation, Second Edition, 1998.

Dauvois, S., Simard, J., Dumont, M., Haagensen, D.E., and Labrie, F. (1990) Opposite effects of estrogen and the progestin RSO20 on cell proliferation and GCDFP-15 expression in ZR-75-l human breast cancer cells. Endocrinology 73, 171-178.

Digital Processing of Signals; Theory and Practice, Edited by M. Bellanger. John Wiley and Sons Ltd., Third Edition, 2000.

Digital Signal Processing; Principles, Algorithms and Applications, Edited by J.G. Proakis and D.G. Manolakis. Prentice-Hall Incorporation, Third Edition, 1996.

Dimitrov, O.A. and Lalchev, Z.I. (1998) Interaction of sex hormones and cholesterol with monolayers of dipalmitoylphosphatidylcholine in different phase state. J. Steroid Biochem. Molec. Biol. 66, 55-61.

Discrete-Time Signal Processing, Edited by A.V.Oppenheim. Prentice-Hall Incorporation, 1989.

Frengeli, U.P. and Günthard, H.H. (1976) Hydration sites of egg phosphatidylcholine determined by means of modulated excitation infrared spectroscopy. Biochim.Biophys.Acta 450, 101-106.

Gottesman, M.M and Fletschmann, R.D. (1986) The role of cAMP in regulating tmour cell growth. Cancer Surv. 5, 291-308.

Gulinello, M. and Smith, S.S. (2003) Anxiogenic Effects of Neurosteroid Exposure - Sex Differences and Altered $GABA_A$-Receptor Pharmacology in Adult Rats. J. Pharmacol Exp Ther., 305(2), 541-548.

Güldütuna, S., Deisinger, B., Weiss, A., Freisleben, H-J., Zimmer, G., Sipos, P., and Leuschner, U. (1997) Ursodeoxycholate stabilizes phospholipid-rich membranes and mimics the effect of cholesterol: investigations on large unilamellar vesicles. Biochim. Biophys. A. 1326, 265-274.

Harness, J.R and Anderson, R.R. (1977) (a) Effect of relaxin in combination with prolactin and ovarion steroids on mammary growth in hypophysectomized rats. Proc. Soc. Exp. Biol. Med., 156, 354-360.

Harness, J.R and Anderson, R.R. (1977) (b) Effect of relaxin and somatotropin in combination with ovarian steroids on mammary glands in rats. Biol. Reprod., 17, 599-604.

Huang, C-H. and Li, S. (1999) Calorimetric and molecular studies of the thermotropic phase behaviour of membrane phospholipids. Biochim.Biophys.Acta 1422, 273-307.

Jacobson, K. and Papahadjopoulos, D. (1975) Phase transitions and phase separation in phospholipid membranes induced by changes in temperature, pH and concentration of bivalent cations. Biochemistry 14, 152-161.

Jain, M.K. and Min Wu, N. (1977) Effect of small molecules on the dipalmitoyl lecithin liposomal bilayer: III phase transition in lipid bilayer. J. Membrane Biology 34, 157-201.

Janiak, M.J., Small,D.M. and Shipley,G.G., The Nature of the Thermal Pretransition of Synthetic Phospholipids: Dimyristol and Dipalmitoyllecithin. Biochemistry, 1976.

Jensen, E.V., Suzuki, T., Kawashima, T., Stumpf, W.E., Junsblut, P.W. and De Sombre, E.R. (1968) A two-step mechanism for the interaction of estradiol with rat uterus. Proc. Natl. Acad. Sci. U.S.A. 59, 632-638.

John SantaLucia, Jr. (1998) A unified view of polymer, dumbbell, and oligonucleotide DNA nearest-neighbor thermodynamics. Proc. Natl. Acad. Sci. USA., 95 (4), 1460–1465.

Juengel,J.L., Meberg,B.M., Turzillo,A.M., Nett,T.M., and Niswender,G.D. (1995) Hormonal regulation of messenger ribonucleic acid encoding steroidogenic acute regulatory protein in ovine corpora lutea. Endocrinology 136, 5423-5429.

Karlson, P., Introduction to Modern Biochemistry, Second Edition. Academic Press 1965.

Kazancı, N., Toyran, N., Haris, P.I., Severcan, F. (2001) Vitamin D2 at high and low concentrations exert opposing effects on molecular order and dynamics of dipalmitoyl phosphatidylcholine membranes, Spectroscopy 15, 47-55.

Koyama, T.M., Stevens, C.R., Borda, E.J., Grobe, K.J. and Cleary D.A. (2000) Characterizing the gel to liquid crystal transition in lipid-bilayer model membranes. The Chemical Educator 5, 1430-1434.

Lee, A.G. (1977) Lipid phase transitions and phase diagrams. II. Mictures involving lipids. Biochim Biophys Acta 14; 472(3-4), 285-344.

Lee,D.C. and Chapman,D. (1986) Infrared spectroscopic studies of biomembranes and model membranes. Biosci. Rep. 6, 235-256.

Lentz,B.R., Y.Barenholz, and T.E.Thompson, (1976), Fluorescence Depolarisation Studies of Phase Transitions and Fluidity in Phospholipid Bilayers 2. Two-Component Phosphatidylcholine Liposomes. Biochemistry 15, 4529-4537.

Leonetti,H.B., Longo,S., and Anasti,J.N. (1999) Transdermal progesterone cream for vasomotor symptoms and postmenopausal bone loss. Obstet. Gynecol. 94 (2), 225-228.

Liang, Y., Belford, S., Tang, F., Prokai, L., Simpkins, J.W. and Hughes, J.A. (2001) Membrane fluidity effects of estratrienes. Brain Research Bulletin 54, 661-668.

Lopez-Garcia, F., Villalain, J., Gomez-Fernandez, J.C. (1993) Infrared spectroscopic studies of the interaction of diacylglycerols with phosphatidylserine in the presence of calcium. Biochim. Biohys. Acta 1169, 264-272.

Lubin Chen, Michael L. Johnson, and Rodney L. Biltonen. (2001) A Macroscopic Description of Lipid Bilayer Phase Transitions of Mixed-Chain Phosphatidylcholines: Chain-Length and Chain-Asymmetry Dependence. Biophys J, 80, 254-270.

Maggi, A. and Perez, J. (1985) Role of female gonadal hormones in the CNS: clinical and experimental aspects. Life Sciences 37, 893-906.

Marbaix, E., Donnez, J., Courtoy, P.J., and Eeckhout, Y. (1992) Progesterone Regulates the Activity of Collagenase and Related Gelatinases A and B in Human Endometrial Explants. Proc. Natl. Acad. Sci. USA. 89 (24), 11789–11793.

Mavarmoustakos, T., Theoropoulou, E., and Yang, D-P. (1997) The use of high-resolution solid-state NMR spectroscopy and differential scanning calorimetry to study interactions of anaesthetic steroids with membrane. Biochim.Biophys.Acta 1328, 65-73.

Mayor, U., Johnson, C.M., Daggett, V., and Fersht, A.R. (2000) Protein folding and unfolding in microseconds to nanoseconds by experiment and simulation. Proc. Natl. Acad. Sci. USA., 97 (25), 13518–13522.

Melchior, D. L., and J. M. Stein. (1976) Thermotropic transitions in biomembranes. Annu. Rev. Biophys. Bioeng. 5:205-238.

Molecular and Cell Biopyhsics, Nossal,R., Lecar,H. Addison-Wesley Publishing Company, 1991.

Molecular Cell Biology, Lodish, H., Berk, A., Zipursky, S.L., Matsudaira, P., Baltimore, D., Darnell, J., Fourth edition. W.H. Freeman and Company 2000.

Momo, F., Fabris, S., Bindoli, A., Scutari, G., and Stevanato, R. (2002) EPR and DSC study of the effects of propofol and nitrosopropofol on DMPC multilamellar liposomes. Current Topics in Biophysics 26, 75-81.

Mueller, P., T.F. Chien, and B.Rudy, (1983), Formation and Properties of Cell-Size Lipid Bilayer Vesicles. Biophys. J. 44, 375-381.

Muneyyirci-Delale, O., Nacharaja, V.L., Dalloul, M., Altura, B.M., Altura B.T. (1999) Serumionized magnesium and calcium in women after menopause. Fertility and Sterility 71, 869-872.

Persson,I., Adami,H-O., Bergkvist,L., et al. (1989) Risk of endometrial cancer after treatment with oestrogens alone and in conjunction with progestogens: results of a prospective study. B.M.J. 298, 147-151.

Pincus, G. (1943) The biosynthesis of adrenal cortical steroids. J. Clin. Endocrinol. Metab. 3, 195-199.

Principles of Biochemistry; General Aspects, Smith,E.L., Robert,L.H., Lehman, I.R., Lefkowitz,R.J., Handler,P. and White,A. Seventh Edit. Mc-Graw-Hill International Editions, 1983.

Regensteiner,J.G., Hiatt,W.R., Byny,R.L., Pickett,C.K., Woodard,W.D., and Grindlay Moore,L. (1991) Short-term efects of oestrogen and progestin on blood pressure of normotensive postmenopausal women. J.Clin.Pharmacol. 31, 543-548.

Reichelt, J., Hemminger, W., (1983) Unexpected problems in the calibration of heat-flux differential scanning calorimeters. Thermochim Acta 69: 59-70.

Reynolds, L.P. and Redmer, D.A. (1992) Growth and microvascular development of the uterus during early pregnancy in ewes. Biol. Reprod. 47, 698-708.

Rylance,P.B., Brincat,M., Lafferty,K., De Trafford,J.C., Brincat,S., Parson,V., and Studd,J.W.W. (1985) Natural progesterone and hypertensive action. Biomolecular J. 290, 13-14.

Sackmann, E. and Trauble, H. (1972) Studies of crystalline-liquid crystalline phase transition of lipid model membranes. II. Analysis of electron spin resonance spectra of steroid labels incorporated into lipid membranes. J. Am. Chem. Soc. 94, 4492-4498.

Sanchez-Bueno, A., Watanabe, S., Sancho, M.J. and Saito, T. (1990) Studies of conformation and interaction of the cyclohexenone and acetyl group of progesterone with liposomes. J. Steroid Biochem. Molec. Biol. 38, 173-179.

Sato, B., Huseby, R.A., Matsumoto, K. and Samuels, L.T. (1979) Molecular nature of interaction of steroids with biomembranes related to androgen bio-synthesis. J. Steroid Biochem. 11, 1353-1359.

Sauborn, B.M., Held, B., and Kuo, H.S. (1976) Hormonal action in human cervix: Specific progesterone binding proteins in human cervix. J. Ster. Biochem 7, 665- 672.

Schneider, F.M., Marsh, D., Jahn, W., Kloesgen, B., and Heimburg, T. (1999) Network formation of lipid membranes: Triggering structural transitions by chain melting. Proc. Natl. Acad. Sci. 96 (25), 14312–14317.

Severcan, F. and Cannistraro, S. (1988) Direct electron-spin resonance evidence for alpha-tocopherol-induced phase-separation in model membranes. Chem. Phys. Lipids 478, 129-133.

Severcan, F., Kazanci, N., Baykal, V., and Suzer, S. (1995) IR and turbidity studies of vitamin E-cholesterol-phospholipid membrane interactions. Bioscience Reports. 15, 221-229.

Severcan, F., Baykal, U., and Suzer, S., (1996) FTIR studies of vitamin E-cholesterol-DPPC membrane interactions in CH_2 region. Fresenius J. Anal.Chem. 355, 415-417.

Severcan, F. (1997) Vitamin E decreases the order of the phospholipid model membranes in the gel phase: An FTIR study. Bioscience Reports 17, 231-235.

Severcan, F., Durmus, H.O., Eker, F., Akınoğlu, B.G., and Haris, I.P. (2000) Vitamin D2 modulates melittin-membrane interactions. Talanta 53, 205-211.

Shaikh, S.R., Dumaual, A.C., Jenski, L.J. and Stillwell, W. (2001) Lipid phase separation in phospholipid bilayers and monolayers modeling the plasma membrane. Biochimica et Biophysica Acta 1512, 317-328.

Spectroscopy, Edited by D.R.Browning. McGraw-Hill Publishing Company London, 1969.

Spectroscopy and Molecular Structure, Edited by G.W. King. Holt, Rinehart and Winston, Inc., 1965.

Synder,R.G. (1967) Vibrational study of the chain conformation in the liquid n-paraffins and molten polyethlene. J. Chem. Phys. 47, 1316-1360.

Tahir, A., Grabielle-Madelmont, C., Betrencourt, C., Ollivon, M. and Peretti, P. (1999) A differential scanning calorimetry study of the interaction of Lasalocid antibiotic with phospholipid bilayers. Cemistry and Physics of Lipids 103, 57-65.

The Physical Chemistry of Membranes, Edited by B.L. Silver. The Solomon Press, 1985.

Theory of Spectroscopy; An Elementary Introduction, Edited by A. Carrington. Thomas Nelson and Sons Ltd., 1973.

Toyran, N., Severcan, F. (2003) Competitive effect of Vitamin D2 and Ca2+ on phospholipid model membranes: an FTIR study. Chemistry and Physics of Lipids 123, 165-176.

Tsuda, K., Kinoshita, Y. and Nishio, I. (2002) Synergistic role of progesterone and nitric oxide in the regulation of membrane fluidity of erythrocytes in humans: an electron paramagnetic resonance investigation. Ameracn Journal of Hypertension 15, 702-708.

Van Osdol, W.W., Ye, Q., Johnson, M.L. and Biltonen, R.L. (1992) Effects of the anesthetic dibucaine on the kinetics of the gel-liquid crystalline transition of dipalmitoylphosphatidylcholine multilamellar vesicles. Biophys. J. 63, 1011-1017.

Villalain, J., Arranda, F.J., Gomez-Fernandez, J.C. (1986) Calorimetric and infrared spectroscopic studies of the interaction of α-tocopherol and α-tocopheryl acetate with phospholipid vesicles. Eur. J. Biochem. 158, 141-147.

Vincent, M., Gallay, J., De Foresta B. and Alfsen, A. (1980) Liposomes in the study of drug activity and immuno-component cell functions. Academic Press, New York, p. 1970.

Visible and Ultraviolet Spectroscopy, Edited by D. Mowthorpe. John Wiley and Sons, 1987.

Whiting K.P., Restall C.J. and Brain P.F. (2000) Steroid hormone induced effects on membrane fluidity and their potential roles in non-genomic mechanisms. Elsevier Life Sciences 67, 743-757.

Wolf, D.E., Maynard, V.M., McKinnon, C.A., and Melchior, D.L. (1990) Lipid Domains in the Ram Sperm Plasma Membrane Demonstrated by Differential Scanning Calorimetry. Proc. Natl. Acad. Sci. USA., 87 (17), 6893–6896.

Yi, P.N. and MacDonald, R.C. (1973) Temperature-dependence of optical properties of aqueous dispersions of phosphatidylcholine. Chem. Phys. Lipids 11, 114-134.

ENERGY LEVEL EQUATIONS

A.1 Rotational Energy Levels

Molecular energy states arise from the rotation of a molecule as a whole and from the vibrations of its constituent atoms relative to one another as well as from changes in its electronic configuration. The lowest energy levels of a diatomic molecule arise from rotation about its center of mass. As in Figure A.1.1, this molecule can be considered as consisting of atoms of masses m_1 and m_2 a distance R apart. Both of the atoms are rotating around an axis passing through their center of mass. The moment of inertia of this molecule is

$$I = m_1 r_1^2 + m_2 r_2^2 \qquad\qquad (A.1.1)$$

where r_1 and r_2 are the distances of atoms from the axis of rotation. Equation (A.1.1) can also be written as

$$I = \left(\frac{m_1 m_2}{m_1 + m_2}\right)(r_1 + r_2)^2 = \mu R^2 \qquad\qquad (A.1.2)$$

where μ is the reduced mass, defined by

$$\mu = \frac{m_1 m_2}{m_1 + m_2} \qquad\qquad (A.1.3)$$

The resulting term in Equation (A.1.2) expresses the rotation of a single particle of mass μ about an axis, which is a distance R apart from the particle.

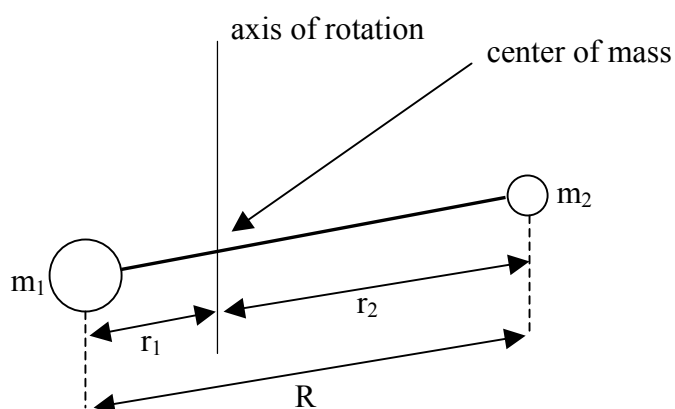
Figure A.1.1 A diatomic molecule rotating its center of mass.

The angular momentum of the molecule has the magnitude

$$L = I\omega \qquad\qquad (A.1.4)$$

where ω is the angular velocity. Solving the radial part of Schrödinger equation leads to

$$L = \sqrt{j(j+1)}\hbar \quad j = 0,1,2,... \tag{A.1.5}$$

where j represents the rotational quantum number and $\hbar$ is a constant defined by

$$\hbar = \frac{h}{2\pi} = 1.054 \times 10^{-34}\,J.s \tag{A.1.6}$$

Thus, angular momentum is quantized in nature.

Energy of the rotating molecule is given by

$$E = \frac{1}{2}I\omega^2 = \frac{L^2}{2I} = \frac{j(j+1)\hbar^2}{2I} \tag{A.1.7}$$

Energy difference between the rotational energy levels is given by the expression

$$\Delta E = E_j - E_{j-1} = \left(\frac{\hbar^2}{I}\right)j \tag{A.1.8}$$

Transition between the rotational energy levels is only possible if a photon of energy ΔE is absorbed by the molecule. The condition for an allowed transition is that

$$\Delta j = \pm 1 \tag{A.1.9}$$

Equation (A.1.9) is also known as the selection rule for allowed transitions.

A.2 Vibrational Energy Levels

Classical approach to a vibrating body of mass m connected to a spring of force constant k gives the frequency of vibration as

$$\nu_0 = \frac{1}{2\pi}\sqrt{\frac{k}{m}} \qquad\qquad\qquad\qquad \text{(A.2.1)}$$

If a molecule is sufficiently excited, it also vibrates. A diatomic molecule can be pictured as if the atoms are connected with a spring of spring constant k, when analyzing the vibrational motion of the molecule (Figure A.2.1). If the system is isolated, namely, a total external force applied to the system is zero, linear momentum of the molecule stays constant. Therefore, the motion of centre of mass is not affected due to the individual vibrations. The frequency of oscillation of such a two-body oscillator is given by Eqn. (A.2.2), where μ is the reduced mass.

$$\nu_0 = \frac{1}{2\pi}\sqrt{\frac{k}{\mu}} \qquad\qquad\qquad\qquad \text{(A.2.2)}$$

Energy of the harmonic oscillator is restricted to some certain values, when the problem is treated quantum mechanically (Ref. Beiser, Sec. 5.9). These quantized energies are given as

$$E_\nu = \left(\nu + \frac{1}{2}\right)h\nu_0 \quad \nu = 0, 1, 2, \ldots \qquad\qquad \text{(A.2.3)}$$

In the above equation, ν is called the vibrational quantum number and it can take integer number values. Equation (A.2.3) can be modified by using Equation (A.2.2), which gives

$$E_\nu = \left(\nu + \frac{1}{2}\right)\hbar\sqrt{\frac{k}{\mu}} \qquad \nu = 0, 1, 2, ... \tag{A.2.4}$$

The selection rule for transitions between vibrational states is $\Delta\nu = \pm 1$
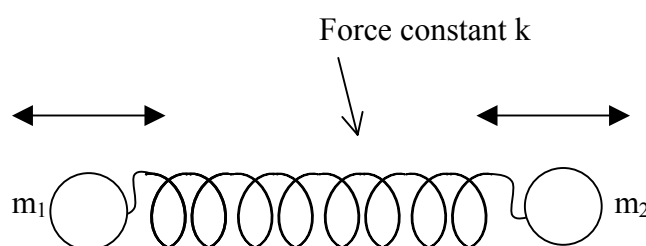
Force constant k

Figure A.2.1 A two-body oscillator. Two bodies of mass m_1 and m_2 are connected with a spring of force constant k.

A.3 Electron Spin

Electron possesses an intrinsic angular momentum independent from the orbital angular momentum. The quantum number s is used to represent the spin angular momentum of the electron. The value of s can only be s = ½ for the electron. S is the magnitude of the angular momentum due to electron spin and it is given in terms of spin quantum number as

$$S = \sqrt{s(s+1)}\hbar = \frac{\sqrt{3}}{2}\hbar \tag{A.3.1}$$

The space quantization of electron spin is described by the spin magnetic quantum number m_s, which can take values $m_s = \pm 1/2$. In the presence of a magnetic field in the z direction, the component S_z of the spin angular momentum of an electron is determined by the spin magnetic quantum number.

$$S_z = m_s \hbar = \pm \frac{1}{2} \hbar \qquad \text{(A.3.2)}$$

Therefore, when there is magnetic field the spin angular momentum vector can have only two orientations as $m_s = \pm 1/2$.

A.4 Nuclear Spin

Nucleus consists of neutrons with no spin and protons with spin ½. Net spin of the nucleus is determined by the spin states that the protons are in and the number of protons present. This spin state of the nucleus is called the nuclear spin quantum number and it is shown by I. In the presence of external magnetic field, there will be (2I + 1) orientations of the nuclear spin. The magnitude of the splitting between the lines is called the hyperfine splitting constant.

APPENDIX B

SIMPLE HARMONIC MOTION

Any motion that repeats itself is called periodic motion or simple harmonic motion. Vibration of a single particle is the most fundamental example of it. A small displacement x from its equilibrium position sets up a restoring force, which is proportional to x and acting in a direction towards the equilibrium position. This restoring force F may be written as

$$F = -sx \qquad (B.1)$$

where s, the constant of proportionality, is called the stiffness and the negative sign shows that the force is acting against the direction of increasing displacement and back towards the equilibrium position. The equation of motion of such a disturbed system is given by the dynamic balance between the forces acting on the system, which by Newton's Law is

$$m\ddot{x} = -sx \qquad (B.2)$$

where m is the mass of the particle and the acceleration is defined as

$$\ddot{x} = \frac{d^2 x}{dt^2} \tag{B.3}$$

Equation of motion can be rewritten as;

$$\ddot{x} + \frac{s}{m} x = 0 \tag{B.4}$$

Here we define the ratio (s/m) as the period of oscillation represented by the symbol T. The reciprocal of T is defined as the frequency shown by υ, with which the system oscillates.

$$T = \frac{1}{\upsilon} = 2\pi \sqrt{\frac{m}{s}} \tag{B.5}$$

However, when the equation of motion is solved, it is found that the behaviour of x with time has sinusoidal or cosinusoidal dependence, it is appropriate to consider the angular frequency ω, defined as;

$$\omega^2 = \frac{s}{m} \tag{B.6}$$

Thus, the equation of motion takes the form

$$\ddot{x} + \omega^2 x = 0 \tag{B.7}$$

In the case of block-spring system, angular frequency is given by

$$\omega = \sqrt{\frac{k}{m}}$$
(B.8)

where k is the spring constant. A two-particle system, consisting of chemically bonded molecules, can be considered as a block-spring system because a chemical bond behaves like spring; there is a restoring force. Since in a two particle case it is difficult to deal with the molecules separately, it is appropriate to use the center of mass system defined as

$$\frac{1}{\mu} = \frac{1}{m_1} + \frac{1}{m_2}$$
(B.9)

where μ is the center of mass or it is also called "reduced mass", m_1 is the mass of the first molecule and m_2 is the mass of the second molecule. Frequency of oscillation is given as

$$\upsilon = \frac{1}{2\pi}\sqrt{\frac{k}{\mu}}$$
(B.10)

APPENDIX C

SIGNALS AND FOURIER SERIES

C.1 Representing Signals

Signals are detectable physical quantities or variables by means of which messages or information can be transmitted. Electrical signals are the most easily measured and the most simply represented type of signals. For example, many physical quantities, such as temperature, humidity, speech, wind speed, and light intensity, can be transformed to time-varying current or voltage signals.

Mathematically, signals are represented as functions of one or more independent variables. As an example; the vibration of a rectangular membrane can be represented as a function of two spatial variables (x and y coordinates).

C.1.1. Continuous-Time and Discrete-Time Signals

One way to classify signals is according to the nature of the independent variable. If the independent variable is continuous, the corresponding signal is called a continuous-time signal and is defined for continuum values of the independent variable. A telephone or a radio signal as a function of time is examples of continuous-time signals.

If the independent variable takes on only discrete values $t = kT_s$, where T_s is a fixed positive real number and k ranges over a set of integers (i.e., k = 0, ±1, ±2, etc.), the corresponding signal is called a discrete-time signal. Discrete-time signals arise naturally in many areas of business, economics, science, and engineering.

Signals can also be classified as analog or digital signals. An analog signal is a physical quantity that varies with time, usually in a smooth and continuous fashion. However, the values of a discrete-time signal can be continuous or discrete. If a discrete-time signal takes on all possible values on a finite or infinite range, it is said to be a continuous- amplitude discrete-time signal. Alternatively, if the discrete-time signal takes on values from a finite set of possible values, it is said to be a discrete-amplitude discrete-time signal, or, simply, a digital signal.

In order to process signals digitally, the signals must be in digital form (discrete in time and discrete in amplitude). If the signal to be processed is in analog form, it is first converted to a discrete-time signal by sampling at discrete instants in time. The discrete-time signal is then converted to a digital signal by a process called quantization.

Quantization is the process of converting a continuous-amplitude signal into a discrete-amplitude signal and is basically an approximation procedure. The whole procedure is called analog-to-digital (A/D) conversion, and the corresponding device is called an A/D converter.

C.1.2. Periodic versus Aperiodic Signals

Any continuous-time signal that satisfies the condition

$$x(t) = x(t + nT) \qquad n = 1, 2, 3, \ldots \qquad\qquad (C.1.2.1)$$

is classified as a periodic signal, where $T > 0$ is a constant known as the fundamental period. A signal $x(t)$ that is not periodic is referred to as an aperiodic signal. Familiar examples of periodic signals are the sinusoidal functions. Since a periodic signal is a signal of infinite duration that should start at $t = -\infty$ and go on to $t = \infty$, it follows that all practical signals are aperiodic.

C.1.3 Signal Filtering

Filtering is the process by which the essential and useful part of a signal is separated from extraneous and undesirable components that are generally referred to as noise. The idea of filtering is based on the convolution property of Fourier transform, namely, the Fourier transform of the output is the product of the Fourier transform of the input and the frequency response of the system. An ideal frequency-selective filter is a filter that passes certain frequencies without any change and stops the rest. The most common types of filters are the low-pass, high-pass, band-pass, and band-stop filters.

High-pass filters are characterized by a stop band that extends from $\omega = 0$ to $\omega = \omega_c$, where ω_c is called the cutoff frequency of the filter, and a passband that

extends from $\omega = \omega_c$ to infinity. However, low-pass filters are those characterized by a passband that extends from $\omega = 0$ to $\omega = \omega_c$, where

Low-pass filters are those characterized by a passband that extends from $\omega = 0$ to $\omega = \omega_c$, where ω_c is called the cutoff frequency of the filter (Fig.C.1.3.1.a). High-pass filters are characterized by a stop band that extends from $\omega = 0$ to $\omega = \omega_c$ and a passband that extends from $\omega = \omega_c$ to infinity (Fig.C.1.3.1.b).
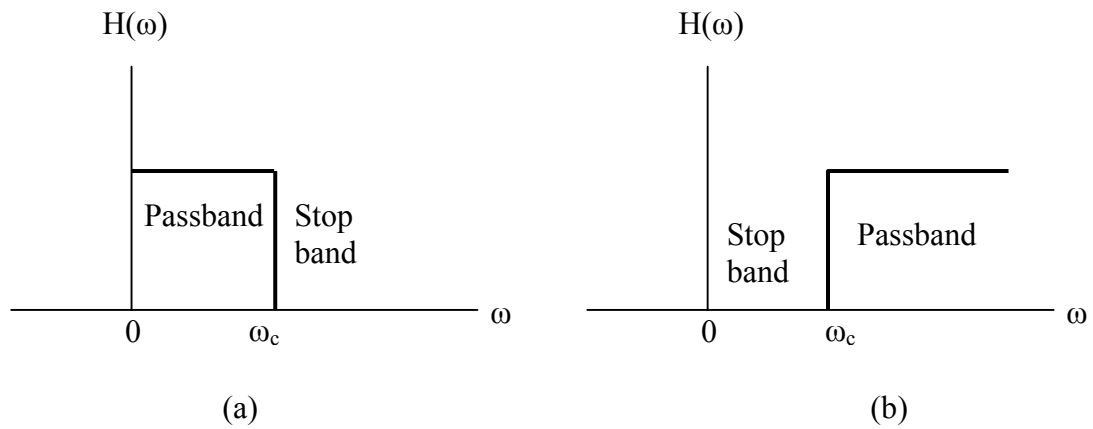

Figure C.1.3.1 Graphical representation of filtering by (a) a low-pass filter and (b) a high-pass filter.

C.2 The Fourier Series

It is possible to obtain the response of a linear system to an arbitrary input by representing it in terms of basic signals. It is convenient to choose a set of orthogonal waveforms as the basic signals. This is because, many of the calculations involving signals are simplified by using such a representation and it is possible to visualize the

signal as a vector in an orthogonal coordinate system, with the orthogonal waveforms being the unit coordinates.

A set of signals φ_i, $i = 0, \pm1, \pm2, \ldots$, is said to be orthogonal over an interval (a,b) if

$$\int_a^b \phi_l(t)\phi_k^* dt = \begin{cases} E_k, & l = k \\ 0, & l \neq k \end{cases} = E_k \delta(l-k) \tag{C.2.1}$$

where $\phi_k^*(t)$ stands for the complex conjugate of the signal and $\delta(l-k)$, called the Kronecker delta function, is defined as

$$\delta(l-k) = \begin{cases} 1, & l = k \\ 0, & l \neq k \end{cases} \tag{C.2.2}$$

If $\phi_i(t)$ corresponds to a voltage or a current waveform associate with a 1-ohm resistive load, then, E_k is the energy dissipated in the load in b − a seconds due to signal $\phi_k(t)$. If the constants E_k are all equal to 1, $\phi_i(t)$ are said to be orthonormal signals. Normalizing any set of signals $\phi_i(t)$ is achieved by dividing each signal by $\sqrt{E_i}$.

Orthonormal sets are useful in that they lead to a series representation of signals in a relatively simple fashion. Let $\phi_i(t)$ be an orthonormal set of signals on an

interval a < t < b, and let *x(t)* be a given signal with finite energy over the same interval. We can represent *x(t)* in terms of $\{\phi_i(t)\}$ by a convergent series as

$$x(t) = \sum_{i=-\infty}^{\infty} c_i \phi_i(t) \qquad (C.2.3)$$

where

$$c_k = \int_a^b x(t) \phi_k^*(t) dt, \quad k = 0, \pm 1, \pm 2, \ldots \qquad (C.2.4)$$

The series representation of Equation (C.4.3) is called a generalized Fourier series of *x(t)*, and the constants c_i, $i = 0, \pm 1, \pm 2, \ldots$, are called the Fourier coefficients with respect to the orthogonal set $\{\phi_i(t)\}$.